5

Formulation Strategies for Pulmonary Delivery of Poorly Soluble Drugs

Nathalie Wauthoz and Karim Amighi
Laboratory of Pharmaceutics and Biopharmaceutics, Faculty of Pharmacy, Université Libre de Bruxelles (ULB), Belgium

Abbreviations

List of Abbreviations

API	Active pharmaceutical ingredient
AUC	Area under the curve
BAL	Broncho-alveolar lavage
BCS	Biopharmaceutical Classification System
BDP	Beclomethasone dipropionate
CD	Cyclodextrin
C_{max}	Maximum concentration
CMC	Critical micelle concentration
C_s	Saturation solubility
CSA	Cyclosporine A
CXB	Celexocib
d_{ae}	Aerodynamic diameter
DPI	Dry powder inhaler
DPPC	Dipalmitoyl phosphatidylcholine
DSPE	Distearoyl phosphatidylethanolamine
DSPG	Distearoyl phosphatidylglycerol
FDA	Food and Drug Administration
FPD	Fine particle dose
GRAS	Generally recognized as safe
HP	Hydroxypropyl
HPH	High-pressure homogenization

Pulmonary Drug Delivery: Advances and Challenges, First Edition. Edited by Ali Nokhodchi and Gary P. Martin.

ITZ	Itraconazole
LNC	Lipid nanocapsule
MMAD	Mass median aerodynamic diameter
Mw	Molecular weight
NSAID	Nonsteroidal anti-inflammatory drug
NLC	Nanostructured lipid carrier
PEG	Polyethylene glycol
PK	Pharmacokinetic
pMDI	Pressurized metered dose inhaler
PTX	Paclitaxel
SBE	Sulfobutylether
SD	Solid dispersion
SLF	Simulated lung fluid
SLN	Solid lipid nanoparticle
TAC	Tacrolimus
Tc	Gel-liquid crystal transition temperature
TEER	Transepithelial electrical resistance
$t_{1/2}$	Half-life
t_{max}	Time for reaching C_{max}
TPGS	Tocopherol polyethylene glycol 1000 succinate
URF	Ultra-rapid freezing
VCZ	Voriconazole

5.1 Introduction

It is estimated that 40% of the currently marketed active pharmaceutical ingredients (APIs) and up to 75% of drugs currently in research and development are poorly water soluble [1]. The poor solubility of the APIs, regardless of the administration route, commonly generates bioavailability or efficacy problems. These issues have been frequently encountered for poorly water-soluble drugs formulated for the oral, as well as intravenous administration [1–3]. Indeed, a drug has to be dissolved before being absorbed through a biological membrane and/or exerting its pharmacological action. A Biopharmaceutical Classification System (BCS) has been developed more specifically for drugs delivered by the oral route, which is based on the solubility/dissolution properties and gastrointestinal permeability of a drug and the resultant drug absorption [4]. It classifies drugs into one of four classes: both highly soluble and permeable (Class I); poorly soluble and highly permeable (Class II); highly soluble and poorly permeable (Class III); and both poorly soluble and permeable (Class IV). Generally, poorly water-soluble drugs within Class II have a higher lipophilicity ($\log P > 0$) and, therefore, high membrane permeability. Therefore, the dissolution of the drug provides the rate-limiting step to absorption. To overcome these issues, strategies to improve solubility/dissolution properties for oral and parenteral routes, including pH adjustment, salt-form selection, control of polymorph, co-crystal formation, particle size reduction, amorphous solid dispersion (SD), the use of co-solvents, surfactants, cyclodextrins (CDs), and lipid-based formulations, are all being used and have been reviewed elsewhere [1–3].

Pulmonary delivery has gained importance in the therapeutic field because of the numerous advantages this route of administration confers, in comparison to the oral or parenteral routes. The API can be delivered directly to the lung in a high concentration to treat respiratory diseases such as asthma, chronic obstructive pulmonary disease, and bacterial or fungal pulmonary infections. For example, the drug delivery strategies for pulmonary administration of antibiotics is described in Chapter 11 and this route could also be considered for treating lung tumors (Chapter 12). The advantages of such localized therapy include a reduction in systemic side-effects and a decreased incidence of potential

drug–drug interactions. These reductions are due to the decrease in systemic drug concentrations, whilst ensuring a therapeutic efficiency that is similar or superior to oral or parenteral delivery. Moreover, pulmonary drug delivery in the gas-exchange zone has been and is being increasingly considered for systemic drug delivery due to the large surface area of the alveolar epithelium (~100 m^2) and the high capillary vascularization upon contact with the very thin alveolar epithelium (~0.2 μm) [5–7]. These characteristics promote systemic absorption while avoiding first-pass effect metabolism and oral bioavailability issues [5–7].

This chapter focuses on the issues associated with pulmonary-delivered poorly water-soluble drugs, defined as drugs presenting an approximate aqueous solubility below 0.1 mg mL^{-1} and considered by Pharmacopoeias as practically insoluble in water at ambient temperature. The *in vivo* fate of poorly water-soluble drugs deposited in the lung and the resulting lung and systemic pharmacokinetics (PKs) are considered. Then, the factors that can be implemented to improve localized, or to optimize the systemic, delivery of such drugs are discussed. Finally, the main formulation strategies for improving lung or systemic delivery of inhaled poorly water-soluble drugs are described.

5.1.1 *In vivo* Fate of Inhaled Poorly Water-soluble Drugs

The impact of the aerodynamic performance, dissolution/solubility properties, and lung permeability of poorly water-soluble drugs on their *in vivo* fate in the lung is illustrated in Figure 5.1.

Undissolved drug particles are cleared by the mucociliary escalator or phagocytized by alveolar macrophages in the conducting or respiratory zone, respectively. Dissolved drug particles can act on their local pharmacological target, or are metabolized by epithelial cells, and are absorbed (either intact or as metabolite) through the lung epithelium into the blood. The resulting lung and plasma PK parameters are illustrated according to the dissolution/solubility properties and the permeability of poorly water-soluble drugs. All lung clearance mechanisms (mucociliary escalator, macrophage phagocytosis, metabolism, and absorption) contribute to the lung half-life ($t_{1/2}$) and area under the curve (AUC) and are determined by the lung-deposited dose. The plasma PK is dependent on the absorption of dissolved drug particles and is characterized in plasma by the maximum concentration (C_{max}), time for reaching C_{max} (t_{max}) and $AUC_{0-\infty}$.

Pulmonary drug delivery consists of drug-based formulations for inhalation aerosolized by an appropriate device. There exist three kinds of devices: nebulizers containing aqueous-based formulations, pressurized metered dose inhalers (pMDIs) for solution or suspension formulations, and dry powder inhalers (DPIs) containing (as the name suggests) dry powders for inhalation [8]. These formulations and functionality of the devices are considered in more detail elsewhere (see Chapter 3). The aerosol, comprising a population of particles/droplets, is carried by the patient's inspiratory airflow into the airways, the actual site of deposition being dependent upon aerodynamic diameter (d_{ae}). This diameter should ideally be controlled within the range of 1–5 μm to maximize the efficiency of lower lung deposition. The aerosol performance of a formulation/device combination is assessed in the principal Pharmacopoeias by determining *in vitro* the fine particle dose (FPD), i.e., the dose of drug particles presenting a d_{ae} lower than or equal to 5 μm, and/or the mass median d_{ae} (MMAD), i.e., the median of the aerodynamic particle size distribution expressed in mass [9, 10]. Particles having a d_{ae} of 3–5 μm are deposited mainly in the conducting zone, whereas particles with a d_{ae} of 1–3 μm are deposited primarily in the respiratory zone [9]. Chapter 1 provides an overview of the role of lung anatomy and physiology in pulmonary drug delivery.

Once inhaled and deposited in the lung, drug particles are in contact with and progressively dissolved (Chapter 10) in the fluid covering the lung epithelium at a velocity determined by the Noyes–Whitney equation [11]:

$$\frac{dM}{dt} = \frac{A \times D \times (C_s - C_t)}{h} \tag{5.1}$$

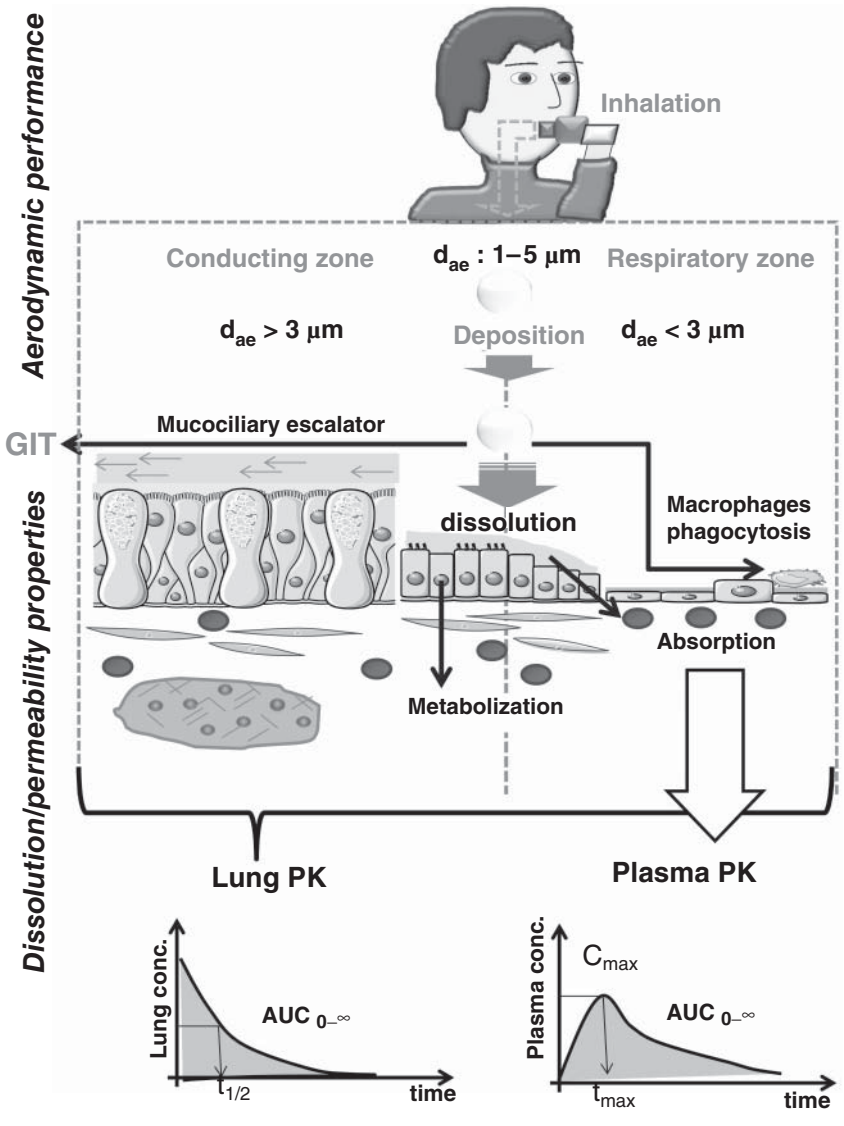

Figure 5.1 *The in vivo lung deposition, dissolution, and fate of poorly water-soluble drug particles in the conducting (d_{ae} >3 µm) or respiratory zone (d_{ae} <3 µm) of the lower respiratory airways*

where dM/dt is the drug solid dissolution rate, A is the surface area of the drug solid in contact with the dissolution medium, D is the diffusion coefficient of drug molecules in the dissolution medium defined by the Stokes–Einstein equation [12], h is the diffusion layer thickness, C_s is the drug saturation solubility at the drug solid surface, and C_t is the drug concentration at time t in the well stirred bulk. The latter is estimated to be negligible under the so-called SINK conditions (i.e., when $C_t \ll C_s$).

The thickness and the composition of lung epithelial lining fluid vary throughout the lower respiratory airways. Indeed, in the conducting zone, the particles/droplets are deposited on a thick

viscoelastic mucus layer (10–30 μm thick in the trachea or 2–5 μm in the bronchia). This layer is supported and carried along by a lower viscosity periciliary layer, allowing efficient mucociliary clearance [13]. The viscous layer of mucus is composed of 95% water, 1% lipids, 1% proteins, 2% glycoproteins (mainly mucins), and 1% inorganic salts [14]. The mucus thickness should be sufficient to immerse drug particles, but the mucus viscosity could impair the drug diffusion in the dissolution medium and, therefore, the drug dissolution rate, as indicated by the application of both the Noyes–Whitney and Stokes–Einstein equations [11, 12]. In the respiratory zone, the particles/droplets are deposited on the lung surfactant overlying the alveolar subphase fluid. The latter presents a thickness of ~0.1–0.2 μm [15]. The lung surfactant is composed of ~80% phospholipids, ~10% neutral lipids, and ~10% proteins [15]. The thickness of alveolar subphase fluid could be insufficient to immerse drug particles, but the tensioactive properties of the lung surfactant could increase the wettability of poorly water-soluble drugs and, therefore, their surface area in contact with the dissolution medium, promoting the drug dissolution, again as indicated by the Noyes–Whitney equation [11, 12]. Despite the very small volume of lung epithelial lining fluid, approximately 10–20 mL/100 m^2, drug dose (in the μg or mg range) is usually dispersed on a very large surface area in the respiratory zone, unlike in the conducting zone (100–120 m^2 vs. 2–3 m^2) [16]. This large surface area allows the absorption of the drug into the blood by diffusion through the thin alveolar epithelium or by active transport [7].

The dissolution rate of drugs in the lung is difficult to assess *in vivo* and indeed, the dissolved fraction is generally estimated indirectly using the absorbed fraction in the blood. Moreover, a standardized *in vitro* dissolution method applicable to lung formulations is very difficult to design because the lung has several unique features such as the small amount of aqueous fluid, the presence of endogenous lung surfactant, and the dispersion of the inhaled formulation onto a very large surface area [10]. A discussion of the assessment of the dissolution of inhaled formulations is provided in Chapter 10.

The rate of dissolution of poorly water-soluble APIs and final proportion dissolved depends on both the wettability and solubility of the drugs in the fluids present in the region where they are deposited. This dissolution process will determine the local lung and systemic PKs and, therefore, the extent of pharmacological action of the drug. Indeed, in the conducting zone (Figure 5.1), undissolved particles are trapped in the mucus, which is progressively removed by the mucociliary escalator to the upper respiratory airways to be swallowed into the gastro-intestinal tract or expectorated [13]. Since the mucus thickness and frequency of ciliated cells decrease along the respiratory airways, mucociliary clearance is less rapid in the peripheral lung, where the rate is estimated to be 1 mm min^{-1} in comparison to 20 mm min^{-1} in the trachea [17]. Consequently, the time taken for elimination by the mucociliary escalator ranges between 2 and 24 h [18]. Under pathological conditions, the lung function might be altered, modifying the deposition and the clearance of the inhaled formulations [5, 19]. In the respiratory zone (Figure 5.1), undissolved drug particles are phagocytized by alveolar macrophages. There are almost 10 macrophages per alveolus patrolling the ~500 billion alveoli constituting the lung [20]. Maximum phagocytosis has been observed for particles in the range of 1–2 μm, with a maximum uptake within 1 h of incubation [21]. Both of these mechanisms (i.e., mucociliary escalator and macrophage phagocytocis) are generally considered as nonabsorptive clearance mechanisms [5]. Nevertheless, once dissolved (Figure 5.1), the drug acts on its pharmacological target (e.g., smooth muscle, site of inflammation or infection, or cancerous cells) in the lung for localized therapy. It is also progressively absorbed (absorptive clearance) into the blood through the lung epithelium at a rate and extent that depends on its absorption mechanism and possible interactions with the lung environment [7]. Drug absorption through the lung epithelium occurs either by passive diffusion, at a rate (F) defined by the following equation, or by saturable active transport [7].

$$F = P \times A \times (C_m - C_0) \tag{5.2}$$

where P is the drug-membrane permeability coefficient, A is the available lung surface area for absorption, C_m is the dissolved drug concentration in the lung lining fluid, and C_0 is the drug concentration on the abluminal side of the membrane. The latter is assumed to be negligible ($C_m \gg C_0$), due to the high blood flow in the lung capillaries.

Small molecules (ranging between 100 and 1000 Da) presenting a log $P < 0$ have a higher $t_{1/2}$ of absorption from the lung to the blood than drugs presenting a log $P > 0$ (~10 min to 1 h in contrast to ~10 s to a few min) [7]. Drugs with a log $P > 0$ are more lipid soluble and are generally assumed to be absorbed transcellularly, whereas drugs with a log $P < 0$ are lipid-insoluble and are assumed to be absorbed paracellularly via aqueous pores in the intercellular tight junctions [7]. These absorptive mechanisms operate by diffusion and are nonsaturable [7]. The rate of absorption by the diffusion of lipophilic drugs is greater in peripheral rather than in central airways due to the decreased thickness and increased surface area of the lung epithelium [7]. The dissolved drug could also be metabolized locally, but generally to a much lower extent than that resulting from the first-pass metabolism that can occur to certain drugs delivered by the oral route [5].

5.1.2 The Pharmacokinetics of Inhaled Poorly Water-soluble Drugs Administered for Local and Systemic Action

The BCS for oral delivery could be partly transposable on pulmonary-delivered drugs for systemic action, where the maximum absorption is required. It might then be possible to correlate absorption with an increase in the solubility/dissolution properties for poorly soluble and highly permeable drugs. However, for drug delivery to the lung, intended to achieve localized effects, this transposition is not applicable. This is because a balance is required between dissolving the sufficient amount of drug to exercise its pharmacological action and limiting the clearance mechanisms to maintain a persistent concentration of dissolved drug in the lung. Therefore, for poorly water-soluble drugs, an improvement in the solubility/dissolution properties and controlled release of such agents may be required so as to optimize localized therapy. Taking all these parameters into account, the modulation of a drug's aqueous solubility and dissolution profile by utilizing formulation technologies could have a direct impact on the lung and systemic PK of the drug and, therefore, on its pharmacological action.

The lung C_{max} and lung t_{max} depend on the time of delivery from the inhalation device. Usually, the concentration and time taken after the end of the inhalation procedure are considered as lung C_{max} and lung t_{max}, respectively. The $t_{1/2}$ of drug in the lung tissue is the pulmonary PK parameter that takes into account all of the clearance systems (i.e., the mucociliary escalator, alveolar macrophage phagocytosis, metabolism, and absorption). The absorption of the dissolved drug into the blood is characterized by the systemic PK parameters, such as the plasma AUC, plasma C_{max}, and plasma t_{max}, as shown in Figure 5.1. The systemic PK parameters depend on the lung tissue permeability and lung fluid solubility (the latter incorporating the dissolution rate as well as C_s) of the drug. The rate of removal by the clearance systems and the permeability and solubility of a poorly water-soluble drug delivered by inhalation are factors that have an impact on the lung residence of the drug. The lung residence is represented by lung AUC. The lung tissue-to-serum concentration ratio is a PK parameter that should be minimized for systemic drug delivery and maximized to obtain high lung retention. However, a balance between the lung retention and the drug absorption has to be found for the localized delivery of poorly soluble and highly permeable drugs.

The PK evaluation of a drug delivered orally, intended for systemic uptake, is relatively easy to perform by blood sampling. However, the PK evaluation for inhaled drug in the lung is rather more difficult. Indeed, plasma PK studies provide poor information about the drug concentrations in lungs after the deposition of the aerosol (i.e., the site where the pharmacological action of the drug might occur in the case of local delivery). This is particularly so for poorly water-soluble drugs, poorly permeable drugs, and slow release formulations [22]. Sampling methods, involving the analysis of drug concentrations in lung tissue homogenates or broncho-alveolar lavages (BALs), are more

suitable for evaluating drug concentrations in the lung but present some inevitable issues. Indeed, lung tissue homogenization sampling does not differentiate between extracellular and intracellular drug concentrations. Furthermore, the BAL method, which gives access to drug concentrations in the epithelial lining fluid, may also injure lung epithelia, resulting in the contamination of the sample with blood components and/or with the contents of disrupted epithelial cells or macrophages. Furthermore, neither method differentiates dissolved, undissolved, and/or carrier-entrapped drug [22, 23].

5.1.3 Formulation Strategies for Pulmonary Delivery of Poorly Water-soluble Drugs

Different classes of drug presenting poor aqueous solubility are used and/or are under evaluation for local drug delivery to the lung. Corticosteroids, such as beclomethasone dipropionate (BDP), budesonide, or fluticasone propionate, were the first poorly water-soluble APIs formulated for inhalation. They are marketed to combat inflammatory processes in asthma and/or chronic obstructive pulmonary disease. In addition, formulations for inhalation containing antifungals such as amphotericin B, itraconazole (ITZ), or voriconazole (VCZ) are under development (Table 5.1). Amphotericin B initially formulated as deoxycholate-based micelles (Fungizone®), liposomes (Ambisome®), or lipid complexes (Abelcet®) for the intravenous route have been tested in clinical trials for inhalation to prevent or combat pulmonary fungal infections such as pulmonary aspergillosis [24]. Indeed, antifungal drugs present poor tissue penetration into lung tissue, severe adverse events, erratic bioavailability, or drug–drug interactions after oral/parenteral administration [25–28]. Inhalation as a route of administration of immunosuppressants such as tacrolimus (TAC) and cyclosporine A (CSA) has been tested in clinical trials in persistent asthma and for lung transplant, respectively, with the aim of decreasing the severe adverse events associated with systemic immunosuppression [24]. The anticancer drug, paclitaxel (PTX) and a nonsteroidal anti-inflammatory drug (NSAID), celexocib (CXB), have been tested to treat lung tumors to maximize the dose in the lung tumors and minimize systemic toxicities [29–32]. Other classes of APIs are also being tested for systemic drug delivery by inhalation. Such drugs include baicalein (a lipoxygenase inhibitor), which has poor aqueous solubility and, therefore, absorption issues (BCS Class II), is subject to extensive intestinal and liver first-pass metabolism, and undergoes enterohepatic circulation when delivered by oral administration [33]. Table 5.1 reports the pharmacological class, physicochemical properties (such as molecular weight (Mw), aqueous solubility, and log *P*), formulation strategies for pulmonary delivery, and respective development status of the poorly water-soluble drugs described in this chapter.

The formulation strategies for poorly water-soluble drugs delivered by inhalation are derived from the strategies for the formulation of similar drugs developed for delivery by the oral or intravenous route. However, the choice of excipients is very limited for pulmonary applications [8] and only a few are approved by the Food and Drug Administration (FDA) (Table 5.2). Only the use of commercially established excipients as well as "generally recognized as safe" (GRAS) substances are promoted by the FDA [8]. This limitation has a direct impact on the choice of excipients for improving the solubility and, therefore, the efficacy of poorly water-soluble drugs for inhalation, and on the commercial potential of the formulations.

5.2 Co-solvents

Co-solvents are miscible organic solvents used to increase the solubility of drugs by modifying the bulk solvent polarity to a level that is closer to the polarity of the drug [1]. Co-solvents such as ethanol (alcohol), glycerin, propylene glycol, or polyethylene glycol (PEG) 600/1000 (Table 5.2) are present, sometimes in a high amount, in aqueous formulations for nebulizers or in propellant-based formulations for pMDI with the aim of increasing the aqueous or propellant solubility of drug, respectively

Table 5.1 *Pharmacological class, physicochemical properties (molecular weight, aqueous solubility and log P), and formulation strategies for pulmonary delivery, with the respective development status reported for the different poorly water-soluble drugs described in this chapter*

Drug	Pharmacological class	Mw g/mol	Aqueous solubility	Log *P*	Formulations for pulmonary delivery	Stage of development
Amphothericin B	Antifungal/ Polyene	924	Practically insoluble[a]; 0.59 mg mL^{-1} [b] 0.25 µg mL^{-1} [34]	0.1 ± 0.9[b]; 1.6 [34]	Surfactant-based micelles (Fungizone®)	Phase III [24]
					Liposomes (Ambisome®)	Phase II/III [24]
					Lipid complex (Abelcet®)	Phase III [24]
Baicalein	Lipooxygenase inhibitor	270.2	0.081 mg mL^{-1} [b]; ~0.1 mg mL^{-1} [33]	3.6 ± 0.5[b]	Nanocrystals	*In vitro* dissolution/*in vivo* PK in rats [33]
Beclomethasone dipropionate (BDP)	Corticosteroid	521.0	Practically insoluble [a]; 0.63 µg mL^{-1} [b]; 0.13 µg mL^{-1} [34]; 0.16 µg mL^{-1} [35]	4.1 ± 0.7[b]; 4.9 [34]	DPI (Qvar®)	Marketed
					Polymeric micelles	*In vitro* dissolution [35]
					Liposomes	γ-scintigraphic study in volunteers [36]
					γ-Cyclodextrins	DPI formulation [37]
Budesonide	Corticosteroid	430.5	Practically insoluble [a]; 9.5 µg mL^{-1} [b]; 16 µg mL^{-1} [34]; 21.5 µg mL^{-1} [38]	3.2 ± 0.6[b]; 3.6 [34]	DPI and Nebulized suspension (Pulmicort®)	Marketed
					Nanoclusters	*In vitro* dissolution [38]
					Polymeric micelles	*In vivo* efficacy on asthma/COPD model [39]
					Solid lipid microparticles	*In vitro* dissolution [40]
					Liposomes	DPI formulation [41]
Celexocib (CXB)	NSAID / COX -2 specific inhibitor	381.4	0.014 mg mL^{-1} [b]; 7 µg mL^{-1} [42]	2.6 ± 0.7[b]; 3.68 [42]	Solid lipid nanoparticles	*In vitro* dissolution/*in vivo* PK in mice [42]
					Co-solvent	*In vivo* efficacy on lung cancer model [32]
Cyclosporine A (CSA)	Immunosuppressant	1203	Practically insoluble [a]; 9.29 µg mL^{-1} [43]; 7.3 µg mL^{-1} [44]	3 ± 1[b]; 2.9 [34]	Co-solvent	Phase II/III [24]
					Liposomes	Phase I [24]
					Surfactant-based micelles	*In vivo* PK in rats [45]
					Solid dispersion	*In vitro* dissolution[46]
					Amorphous nanocrystals	*In vitro* dissolution/*in vivo* PK in mice [47]
					Nanocrystals in hydrophilic carrier	*In vitro* dissolution [48]

Fluticasone propionate	Corticosteroid	500.6	Practically insoluble [a]; 1.4 μg mL^{-1} [b]	3.1 ± 0.6[b]	DPI and Suspension Nebulization (Flixotide®)	On the market
Itraconazole (ITZ)	Antifungal/Azole	706	Practically insoluble [a]; 0.13 μg mL^{-1} [b]; 1 ng mL^{-1} [34, 50]	5.0 ± 0.8 [b]; 5.7 [34]; 6.2 [51]	Nanoclusters	*In vitro* dissolution [49]
					Solid lipid nanoparticles	*In vitro* dissolution [50]
					Nanocrystals/solid dispersion	*In vitro* dissolution/*in vivo* PK in rats [51]
					Nanocrystals	*In vivo* PK in rats [52]
					Nanocrystals in hydrophilic carrier	*In vitro* dissolution [53]
					Solid dispersions	*In vitro* dissolution/*in vivo* PK in mice [54–57]
					HP-β-cyclodextrin/solid dispersion	*In vitro* dissolution/*in vivo* PK in mice [58]
Paclitaxel (PTX)	Anticancer	854	Practically insoluble [a]; 0.24 μg mL^{-1} [b]; <0.01 mg mL^{-1} [60]	3.9 ± 0.8 [b]; 3.96 [60]	Polymeric micelles	*In vitro* dissolution [59]
					Surfactant-based and polymeric micelles	*In vitro* dissolution/*in vivo* PK in rats [61]
					Nanoclusters	*In vitro* dissolution [62]
					Liposomes	*In vivo* PK and efficacy on lung tumors model [29]
					Lipid nanocapsules (LNCs)	LNC formulation/ nebulization [63]
					Solid lipid nanoparticles	*In vivo* efficacy on lung cancer model [30]
Tacrolimus (TAC)	Immuno-suppressant	804	0.018 mg mL^{-1} [b]	4.8 ± 0.9 [b]	Not defined	Phase II [24]
					Nanoclusters/solid dispersion	*In vitro* dissolution/*in vivo* PK in mice [64]
Voriconazole (VCZ)	Antifungal / Azole	349.3	0.042 mg mL^{-1} [b]; 0.7 mg mL^{-1} [65]	1.2 ± 0.8[b]; 1.8 [65]	Nanoclusters/solid dispersion	*In vitro* dissolution/*in vivo* PK in mice [65]
					SBE-β cyclodextrin	*In vivo* PK in mice [66]

[a] Data from the European Pharmacopoeia.
[b] Calculated using the advanced chemistry development software, V11.02.

Table 5.2 *List of excipients from functional classes useful for formulating poorly water-soluble drugs and that are approved, commercially established, "GRAS", or have good potential for inhalation*

Excipient		Dose (inhalation device used)	Status
Lipid	Cetyl alcohol	9.4% (intratracheal instillation)	API in Exosurf®
	Dipalmitoyl phosphatidylcholine (DPPC)	NA[a]	"GRAS": major and endogenous phospholipid of lung surfactant API in Exosurf®
	Distearoyl phosphatidylcholine (DSPC)	NA (DPI)	Commercially established - Tobi Podhaler® (Pulmospheres®)
	Cholesterol		"GRAS": endogenous neutral lipid of lung surfactant
Polymer	Povidone K25	0.0001% (pMDI)	Approved by FDA [67]
	Polyvinylpyrrolidone K30	NA (pMDI)	Commercially established - Lomudal®
	Tyloxapol	6.25% (intratracheal instillation)	API in Exosurf®
Solvent	Alcohol (deshydrated)	10–95.89% (pMDI), 0.081–25% (nebulizer)	Approved by FDA [67]
	Glycerin	7.3% (nebulizer), 0.013% (DPI)	Approved by FDA [67]
	Polyethylene glycol 1000	0.0224% (pMDI)	Approved by FDA [67]
	Polyethylene glycol 600	NA (pMDI)	Commercially established - Lomudal®
	Propylene glycol	25% (NA)	Approved by FDA [67]
Sugar	Glucose	NA (DPI)	Commercially established - Bronchodual®
	Lactose, anhydrous	0.1161%	Approved by FDA [67]
	Lactose, monohydrate	2–9%, 20–25 mg (DPI)	Approved by FDA [67]
	Mannitol	0.051% (DPI) 100% (DPI)	Approved by FDA [67] API in Aridol®
	Trehalose		Good potential [8]
Surfactant	Bile salts		Good potential [8]
	Lecithin soybean	0.0002–0.1% (pMDI)	Approved by FDA [67]
	Lecithin, hydrogenated soybean	0.28% (pMDI)	Approved by FDA [67]
	Polysorbate 20	NA (nebulizer)	Commercially established - Flixotide®
	Polysorbate 80	0.02% (nebulizer)	Approved by FDA [67]
	Oleic acid	0.0003–0.267% (pMDI)	Approved by FDA [67]
	Sorbitan laurate	NA (nebulizer)	Commercially established - Flixotide®
	Sorbitan trioleate	0.0694% (NA)	Approved by FDA [67]

[a]NA: Data not available.

[8]. For propellant-based formulations, the presence of a co-solvent could influence the aerodynamic particle size distribution of the droplets [68]. For dry powders for inhalation, a volatile co-solvent could be used during the production process when they are elaborated by spray-drying [8]. An appropriate co-solvent mixture could increase the solubility of the poorly water-soluble drug by several orders of magnitude, as described by the extended Hildebrand and log-linear solubility equations [69]. These log-linear solubility relationships between the solubilized drug concentration and the co-solvent concentration also implicitly indicate that the solubilizing power of the formulation is rapidly lost and precipitation can occur when the formulation is introduced into and, therefore, diluted by an aqueous media [1]. In addition to such a risk of API precipitation, the inclusion of co-solvents also presents tolerability issues for the pulmonary tissues, according to the nature and the amount of the co-solvent. Moreover, if employed at higher concentrations, then problems of high tonicity can result.

CSA is defined as a Class II drug by the BCS [70], having an aqueous solubility of about 10 μg mL^{-1} (Table 5.1). CSA was first delivered by inhalation in animal models as a hydro-alcoholic solution using ethanol as co-solvent [71]. Due to the irritating effect of ethanol preparations on the respiratory tract, a propylene glycol solution of CSA was prepared to provide a concentration of 62.5 mg mL^{-1} to enable a dose of 300 mg to be delivered by nebulization in most clinical studies [71]. Propylene glycol also causes significant irritation of the airways, so the pretreatment of the patient with aerosolized local anesthetic and bronchodilator is required [72]. Burkart *et al*. observed a rapid initial absorption of CSA over the first 4–6 h, followed by a slower, sustained complete absorption over a prolonged period of 24 h after the delivery of a propylene glycol solution of CSA to the transplant patients' lungs by nebulization [73]. On the one hand, Trammer *et al*. showed that the permeability of the CSA through the human bronchial adenocarcinoma cell Calu-3 monolayer remained unaltered by the inclusion of propylene glycol [72]. However, it was assumed that the propylene glycol freely permeated the lung due to its physicochemical properties (low molecular weight and surface tension, log *P* of −0.79, water miscibity, and molecular radius below that of the tight junction pores) [44] and it was these characteristics that promoted the precipitation of CSA in the lung fluid. Therefore, the solubility could again have become the rate-limiting dissolution process, influencing directly the rate of absorption of CSA through the lung. The initial, rapid absorption observed *in vivo* could correspond to the solubilized fraction of CSA, which decreased progressively because of the dilution of the formulation in the lung fluid and the continual permeation of propylene glycol through the lung (and hence removal from the applied co-solvent), which leads to the precipitation of CSA. The novel dynamic equilibrium between the solubilized and nonsolubilized fractions of precipitated CSA (acting as a reservoir) could explain the slower, prolonged phase of absorption of the drug as it was solubilized progressively from the nonsolubilized fraction. All drug deposited in the lung was systemically absorbed [73], revealing no problem of permeability of CSA through the lung, in spite of its high molecular weight.

5.3 Cyclodextrins

Cyclodextrins (CDs) are extensively described in several reviews [1, 74, 75]. Briefly, CDs are cyclic oligosaccharides derived from starch consisting of covalently (α-1,4) linked α-D-glucopyranose units. The most common – αCD, βCD, and γCD – contain six, seven, and eight units, respectively. CDs have a morphology analogous to truncated cones with a hydrophilic outer exterior and a hydrophobic inner interior presenting a polarity close to that of a hydro-ethanolic solution. CDs enhance the apparent aqueous solubility and modify the physical and chemical stabilities and other physicochemical properties of drugs. They do so mainly by the formation of a noncovalent inclusion complex, where the guest molecules (drug) and the host molecules (CDs) are in dynamic equilibrium. The guest or a part of it has to present a suitable size and polarity to be included in

the cavity of the corresponding CD. Generally, an increase in the aqueous solubility of 10-fold to 1000-fold is often seen when a CD concentration of 0.1 M is used, and even higher increases can occasionally be observed [75]. Some CDs, such as βCD, present a limited aqueous solubility and, therefore, can induce nephrotoxicity due to precipitation occurring in the glomerular filtrate. To increase aqueous solubility, derivatives have been synthetized such as: dimethyl-βCD, hydroxypropyl (HP) βCD, sparingly methylated βCD (Crysmeb), randomly methylated βCD (Rameb), sulfobutylether (SBE) βCD, and the so-called branched CDs, such as maltosyl-βCD. Drug release from CDs generally occurs in a solution according to the dissociation constant of the complex and as a result of simple dilution. Release can also be triggered by the replacement of the included guest with some other suitably sized molecule (including lipids from the cell membrane or lung surfactant such as cholesterol or phospholipids), or because the included guest has a higher affinity to proteins or lipophilic membrane than to the CDs. In terms of CD permeability through the lung tissue, CDs alone or CD complexes are considered unable to cross cell layers. The permeability of CDs through Calu-3 cell layers is close to 7×10^{-8} cm s^{-1} for αCD, βCD, and γCD [76]. However, Marques *et al*. have reported an *in vivo* systemic bioavailability of radiolabeled CDs delivered intratracheally in rabbit lung of 66% for βCD and 74% for both dimethyl-βCD and HP-βCD [77].

In addition to enhancing aqueous solubility, CDs could modify the permeability of drug through membranes by acting as permeation enhancers. Salem *et al*. [78] and Matilainen *et al*. [76] have shown that CDs (Rameb, Crysmeb, HP-βCD, HP-γCD) did not influence the paracellular transport of mannitol when each was added concurrently with the monosaccharide to a Calu-3 cell monolayer. However, after 4 h exposure to the different CDs, a change in mannitol permeability was observed for Rameb (beginning at a 10 mM concentration of the CD), Crysmeb and HP-βCD (at 25 and 50 mM, respectively), whereas no change was observed for HP-γCD (up to the highest concentration of 50 mM) [78]. The transepithelial electrical resistance (TEER) is a measure of functional tight junctions of the Calu-3 monolayer and, therefore, of the permeability to paracellular transport [79]. The final TEER of the Calu-3 monolayer decreased with the CD concentration, increasing the permeability of mannitol. The initial TEER was recovered within 24 h after exposure, except for concentrations >10 mM of Rameb, which caused an irreversible TEER decrease [78]. The absorption enhancement ability of CDs is often considered in relation to their ability to extract membrane lipids, which is also related to their low biocompatibility. The affinity of CDs to cholesterol increases in the order of βCD = γCD = HP-γCD = SBE-βCD < HP-βCD < Crysmeb < Dimeb < Rameb = Trimeb; for soybean phospholipid, it increases in the order of βCD = γCD = HP-γCD = SBE-βCD < HP-βCD < Crysmeb < Trimeb < Rameb < Dimeb [80]. However, Evrard *et al*. have evaluated the short-term toxicity (daily for seven days) of different CDs (HP-βCD, γCD and Rameb) delivered by the inhalation route – specifically, by nebulization – in mice. No histological changes in the lung (integrity of epithelium and inflammation score) and no bronchial responsiveness were observed after one week of daily inhalation [81]. However, a slight increase in lymphocytes in BAL was observed in mice exposed to 20 mM of HP-βCD and all doses tested for γCD (20–100 mM) but not those tested for Rameb (20–75 mM) [81]. To date, no CD has been approved as an excipient for inhalation by the FDA and no product for inhalation containing CDs is available on the market (Table 5.2). However, the feasibility of including CDs in nebulizers, pMDIs, or DPIs does remain an option.

VCZ is defined as a Class II drug by the BCS, although it is just at the limit of being categorized as a Class I [65], due to its relatively high aqueous solubility ~0.7 mg mL^{-1} (Table 5.1). VCZ has been complexed with SBE-βCDs (Captisol®), intended for the intravenous route (Vfend®), but this solution was nebulized at a low or high flow rate in the mouse lung [66]. The lung and plasma t_{max} were of 10 and 20 min or 30 and 30 min following a low or a high flow rate of nebulization, respectively [66]. After 6–8 h, either only a low concentration or no VCZ was detectable in the lung tissue, suggesting a rapid absorption of the highly permeable VCZ through the lung epithelium. However, these results are more relevant to employing the inhalation route for systemic drug delivery rather than for localized delivery.

ITZ, presenting a much lower aqueous solubility than VCZ (Table 5.1), was solubilized with HP-βCD, or formulated as an SD using ultra-rapid freezing (URF-ITZ) (see Section 5.6 for more details) and delivered by nebulization in mice [58]. The overall concentration of CDs that could be employed was limited by the requirement to avoid an excessive solution viscosity and to generate a suitable aerosol by a nebulizer. The ITZ solubility increased from 10 ng mL^{-1} (crystalline ITZ) to a maximum of 0.27 mg mL^{-1} with URF-ITZ in simulated lung fluid (SLF) at 37°C [51] or from 1 ng mL^{-1} (crystalline ITZ) to 5.3 mg mL^{-1}, with 15% HP-βCD and amorphous ITZ, in water at 25°C [58]. These solubility levels remained stable over time only for the CD solution, due to the ability of the CDs to inhibit some underlying growth mechanisms of the crystalline drug. The mechanism of inhibition of CDs may include (i) hydrogen bonding to sites associated with crystal growth, (ii) accumulation in the unstirred water layer resulting in an increase in viscosity and hence diffusional resistance, and (iii) complexation of the CD with drug monomers inhibiting efficient mass transfer at the interface [74]. PK data revealed a much faster systemic absorption (plasma t_{max} 1.5 h vs. 3.0 h) and slower lung elimination (lung $t_{1/2}$ 30.9 h vs. 28.0 h) of ITZ from an HP-βCD solution in comparison to a dispersion of URF-ITZ nanoparticles. Indeed, ITZ from an HP-βCD solution was immediately available as a solute for absorption and did not require a prior dissolution step, unlike that from URF-ITZ nanoparticles. However, the serum C_{max} and $AUC_{0-\infty}$ were higher for URF-ITZ than for the HP-βCD solution. This could be due to the presence of lecithin in the URF-ITZ formulation, which could act to promote lung ITZ permeability compared to that induced by HP-βCD. It seems that the modulation of the permeability of ITZ through the lung tissue affected its bioavailability more than the resultant increase in the aqueous solubility.

5.4 PEGylation

PEGylation is the covalent bonding of a PEG molecule to a drug or an excipient. PEG is a polymer that is composed of a covalently bonded repeating structure of ethylene glycol. Each ethylene glycol residue is hydrated by two molecules of water, rendering it highly hydrophilic. Bonding PEG to a drug with a hydrolysable bond produces a pro-drug, with changes in the drug's physicochemical properties. Such changes can include an increased molecular weight and aqueous solubility, and decreased tissue permeability and immunogenicity [82]. Anticancer drugs or proteins have been PEGylated for parenteral administration and have been tested *in vivo*. The resultant benefits of this process have included: an increase in apparent aqueous solubility, increased blood $t_{1/2}$ due to reduced kidney clearance (for PEG conjugates higher than 20 kDa), protection against enzymatic degradation or reduced uptake by the reticulo-endothelial system due to polymer steric hindrance, prevention of immunogenicity of heterologous proteins, and selective tumor accumulation [83]. However, some limitations have also been encountered, such as poor drug loading being achieved and the relatively low availability of suitable groups on the polymer for drug coupling, which have limited the use of this strategy for low molecular weight drugs [83]. Therefore, PEG conjugation to drug is more focused on peptides or proteins mainly delivered by the intravenous route [84]. It has also been examined as a strategy for the systemic delivery of insulin [85] and salmon calcitonin [86] by inhalation. The PEGylation of insulin and salmon calcitonin (both hydrophilic polypeptides) provides protection against degradation by proteolytic enzymes, slows absorption by pulmonary epithelium, and prolongs circulating time in the systemic compartment [82, 86]. To our knowledge, no PEGylation of a poorly water-soluble drug has been evaluated for inhalation. This is despite the possibility that it could increase the water solubility and decrease the permeability of drug and, therefore, the absorptive clearance process, but it could also decrease the recognition of the drug particles by macrophages and, therefore, the nonabsorptive clearance process. Indeed, phagocytosis is enhanced by a charged or hydrophobic surface [87]. PEG conjugation (typically with a PEG having a 2–5 kDa Mw) to an excipient or

carrier (liposomes, lipid nanocarriers, nanoparticles, nanocapsules, micelles, etc.) is widely used to reduce opsonization and recognition of the latter by the reticulo-endothelial system and slow elimination [88]. Moreover, such 200-nm-sized nanoparticles have recently been reported to increase lung mucus penetration [89]. PEGylated carriers used to encapsulate drug and then delivered by inhalation are discussed further in other sections of this chapter. PEG molecules with a 3350 Da Mw are relatively well tolerated, no effects being observed at doses of 109–567 μg L^{-1} for 6 h/day, 5 days/week for two weeks by aerosol therapy in F-344 rats [90]. PEG is accepted as an inactive ingredient by the FDA (Table 5.2) and has been included as an excipient in a pMDI inhaler formulation, but no PEGylated poorly water-soluble API has been reported for pulmonary delivery.

5.5 Reduction of Size to Micro-/Nanoparticles

Particle size reduction can be performed by top-down methods, such as milling or high-pressure homogenization (HPH), or by bottom-up technologies such as precipitation/crystallization methods, as well as a combination thereof [91]. Micronization results in the reduction of particles to a size range of 2–5 μm [1]. Particle size reduction increases the specific surface area (area per unit of mass) and, therefore, the drug dissolution rate, as described by the Noyes–Whitney equation (Equation 5.1). This improvement is increased dramatically when reducing the size to the nanometer scale (<1 μm), where the dissolution velocity is related not only to an increase in the specific surface area but also an increase in the C_s. Indeed, the aqueous solubility of smaller particles is higher than that of large particles, as defined by the Ostwald–Freundlich equation [91]. The explanation was extrapolated from the Young–Laplace and Kelvin equations, where vapor pressure increases above a curved liquid surface in comparison to a flat liquid surface. In the case of a solid in a liquid, when the size decreases, the particle surface curvature increases and therefore the "dissolution pressure" of the drug particles in the dissolution medium increases [91].

Currently, mainly micronized API-based dry powders for inhalation exist on the market and, more specifically, for poorly water-soluble drugs such as BDP, budesonide, and fluticasone propionate (Table 5.1). Some suspensions for nebulization exist with micronized budesonide, or fluticasone propionate (Table 5.1), but these can present some nebulization issues [92]. Usually, micronized drugs in the respirable size range are highly cohesive and require a mixing with coarse carrier, usually lactose (Chapter 7) particles (50–100 μm), to improve the flow/dispersion properties [9]. During the inhalation and aerosol generation through the DPI, a portion of the micronized drugs is dispersed from the carrier surface and deposited in the respiratory tract [9]. Nanoparticles comprise particles with diameters below 1 μm and are, therefore, theoretically exhaled. Indeed, 1 μm is the lower limit for lung deposition by sedimentation [9]. However, nanoparticles are much more highly cohesive than microparticles and are not individually dispersed. Therefore, nanoparticles need to be delivered to the lung either as a suspension by nebulizers or as a dry powder formulation by DPI [93]. Indeed, nebulizers generate aerosol droplet of sizes 1–5 μm that ideally contain the nanoparticles in non-aggregated and well-stabilized suspension. Moreover, nanoparticles may also be delivered by DPI but require presentation as microparticles, where nanoparticles are embedded in a matrix or as micron-sized agglomerates of nanoparticles (nanoclusters), for example [93]. A dry state is often better for storage prior to pulmonary delivery since this reduces the potential for physical and chemical instabilities (such as aggregation or drug leakage) [93]. In the lung, particle size does not appear to influence clearance by the mucociliary escalator [13] but can influence alveolar macrophage clearance. For the latter, maximum phagocytosis is observed for particles of 1–2 μm and minimum phagocytosis for particles above 6 μm or under 0.3 μm [94]. However, for macrophage phagocytosis, the surface properties of particles, such as hydrophobicity and charge, seem to be more important than the particle size [21].

5.5.1 Nanocrystal Suspension

Nanocrystals are composed only of drug in the crystalline state [91]. In such formulations, the presence of a surfactant is required to stabilize the very large surface area of nanocrystals in aqueous media [91].

ITZ as indicated above is categorized as a Class II drug within the BCS [70], having an extremely low aqueous solubility of 1 ng mL^{-1} (Table 5.1). ITZ has been formulated as a suspension of nanocrystals stabilized with polysorbate 80 in water using a top-down wet-milling process, attaining a size of approximately 200 nm [52]. The nanosuspension was then nebulized in rats and produced a lung C_{max} of 21.4 ± 2 $\mu g/g_{wet\ tissue}$ (mean ± SEM), which decreased to 3.0 ± 0.6 $\mu g/g_{wet\ tissue}$ after 72 h, with a lung $t_{1/2}$ of 25.4 h and a lung $AUC_{0-\infty}$ of 829 μg h g^{-1}. Serum concentration increased immediately from 58 ± 2 ng mL^{-1} post-administration to 104 ± 11 ng mL^{-1} 4 h after the inhalation of the suspension, showing a rapid drug absorption from the ITZ nanoparticles which had been solubilized by the lung fluid. A decrease in serum levels to below the analytical limit of quantification was monitored over 36 h, corresponding to a serum $t_{1/2}$ of 10.5 h. The lung tissue-to-serum concentration ratio decreased from 457 to 166 during the rapid absorption of solubilized ITZ (i.e., 1–4 h after inhalation). It then increased up to 528 after 24 h, indicating retention and slow release of ITZ from the remaining ITZ nanoparticles acting as a reservoir in the lung tissue. These results gave a lung $t_{1/2}$ that was superior, overall, compared to the serum $t_{1/2}$ over 24 h. The serum concentrations are related to the absorption of solubilized ITZ from the lung for the major part, and are also attributable to a component that results from the swallowed portion of the dose, cleared by mucociliary clearance and absorbed through the gastro-intestinal epithelium. Rundfeldt *et al*. [52] also evaluated the PKs of ITZ in serum and lung after the oral administration of the same ITZ nanosuspension dose to both fasted and fed rats. The serum t_{max} was observed after 4 h or 12 h, with values of serum C_{max} being 64 ± 14 ng mL^{-1} and 84 ±8 ng mL^{-1} in fed or fasted rats, respectively. The concentrations then remained reasonably stable until 24 h after dosing. Lung tissue paralleled the serum concentration, with similarly stable lung-tissue-to-serum concentration ratios of 3–5:1 being generated [52]. However, these lung concentrations remained 35–70 times less than the lung concentration obtained after the pulmonary administration of the ITZ nanosuspension for a similar serum concentration level. The swallowed part comprises a relatively small portion of the administered dose of the drug in comparison to the solubilized part absorbed from the lung, as shown by the high lung tissue-to-serum concentration. Nevertheless, the existence of this swallowed amount could have led to a slight overestimation of the serum concentrations. Briefly, it seems that nanoparticles of ITZ are able to supersaturate the lung fluid, leading to a rapid absorption of the solubilized part over the first 4 h. However, from 4 h to 24 h, this solubilized fraction decreased in concentration since the remaining nanoparticles were apparently dissolved at a slower rate, as revealed by the slower absorption profile. This observation can also be partly explained by the decrease in the C_s of ITZ nanoparticles over time. A dissolution test, effected in supersaturate conditions, showed that dry ITZ nanocrystals supersaturated an SLF by reaching a concentration value corresponding to threefold the C_s of bulk micronized ITZ (i.e., C_s = 8 ng mL^{-1} in SLF at 37°C) at 30 min. This concentration then decreased to twofold at 6 h and declined to the equilibrium ratio at about 24 h [51]. However, these *in vitro* tests differ greatly from the conditions that prevail *in vivo*, where dissolution and elimination processes coexist.

Baicalein, although regarded as a poorly water-soluble drug, has a much higher aqueous solubility than CSA (~10 μg mL^{-1}) or ITZ (1 ng mL^{-1}), i.e., ~0.1 mg mL^{-1} (Table 5.1). Baicalein has been produced as a suspension of nanocrystals, characterized by a Z-average size of 335 ± 18 nm [33]. This was achieved employing a bottom-up-modified antisolvent recrystallization as a pretreatment procedure, followed by the use of a top-down HPH technique, involving the stabilization of the suspension with polysorbate 80. Particle size reduction increased the dissolution velocity drastically, with almost 100% of baicalein released and dissolved after 15 min from nanocrystal suspension in

comparison to almost 29% after 60 min from the suspension made from the initial baicalein (particle size range 20–160 μm) batch stabilized with the same amount of polysorbate 80. This improvement in the rate of dissolution produced a higher plasma C_{max}, (increasing from 1.9 ± 0.6 μg mL^{-1} to 9.5 ± 0.9 μg mL^{-1}), and shorter t_{max}, (decreasing from 0.139 to 0.083 h) after the pulmonary delivery (intrathecal instillation) of a nanocrystal suspension, in comparison to that generated by a suspension of the initial crystals. Moreover, the plasma PK parameters (t_{max}, C_{max}, and AUC_{0-t}) were not significantly different ($p > 0.05$) from that obtained employing the same dose (10 mg kg^{-1}) delivered intravenously as a PEG 400 solution [33]. The improvement of dissolution/solubility properties from the size reduction allowed baicalein to dissolve almost instantly in lung fluid, the dissolved baicalein being absorbed directly in the blood at a rate comparable to a solution delivered by the intravenous route. Such an absorption profile is generally that which is desired for systemic drug delivery by inhalation, where fast onset of action is required.

The reduction in size of poorly water-soluble drugs below 1 μm increases the surface area and the C_s of drug particles. Therefore, the dissolution rate increases drastically, as does the proportion of dissolved drug that can exert its local pharmacological action and/or be absorbed through the lung epithelium. However, dependent upon the drug's level of aqueous insolubility, the resulting dissolution/solubility properties generate an equilibrium between the proportions of dissolved and undissolved drugs. This equilibrium might provide an appropriate means to control the release of highly permeable drugs for not only local but also systemic drug delivery.

5.5.2 Nanocrystals in a Hydrophilic Matrix System

A hydrophilic excipient may be a key component of a nanoparticle-based dry powder for inhalation produced by spray-drying. The resultant hydrophilic matrix system could help to redisperse nanoparticles from the dry powder into aqueous media and could create a hydrophilic microenvironment around the nanoparticles, limiting agglomeration and increasing the dissolution rate.

Nanocrystals of ITZ (Table 5.1) have been generated from micronized ITZ (mean $d(0.5)$ of 4.79 ± 0.01 μm) by HPH, using tocopherol polyethylene glycol 1000 succinate (TPGS) as a stabilizer in a hydro-isopropanolic solution as the dispersant medium [53]. The particle size distribution of the nanosuspension was characterized as having a mean diameter $d(0.5)$ of 0.221 ± 0.010 μm and a $d(0.9)$ of 1.676 ± 0.007 μm after 300 cycles of homogenization at 20 000 PSI. The ITZ nanocrystals were spray-dried in solutions of mannitol containing the suspension of ITZ nanocrystals with or without additional charged surfactant (i.e., sodium taurocholate) to obtain dry powders for inhalation. The dry powder formulation including mannitol and sodium taurocholate presented the best redispersion of nanoparticles in an aqueous solution, with a $d(0.5)$ of 0.25 ± 0.01 μm and a $d(0.9)$ of 1.77 ± 0.01 μm, and good aerodynamic performance (producing an FPD related to the nominal dose of 50.2 ± 0.6%). Moreover, this dry powdered matrix increased the ITZ C_s from <10 ng mL^{-1} obtained from micronized ITZ to 58 ± 2 ng mL^{-1}, i.e., at least 5–6 times ITZ C_s. The supersaturation solubility decreased over time to ~20 ng mL^{-1} after 3 h due to "nanoparticle instability" in aqueous media. Indeed, this instability was observed by laser diffraction during particle-size analysis, where a new population of approximately 10 μm particles was observed and the original nanoparticle population decreased over time. These changes indicated nanoparticle agglomeration and/or Ostwald ripening, which were more pronounced as the particle size decreased [53]. Indeed, a slight nanoparticle agglomeration could be more favorable in terms of C_s stability over time. Dry powders produced by spray-drying ITZ nanosuspensions, with mannitol containing either no or insufficient sodium taurocholate produced partly irreversible ITZ nanoparticle agglomeration. This agglomeration led to microsized and submicrosized ITZ agglomerates in the aqueous solution (mean $d(0.5)$ of 0.78–1.51 μm). In the dissolution medium, these latter formulations showed higher (87–96 mg mL^{-1} vs. 58 mg mL^{-1}, respectively) and more stable C_s values over time, when compared to the dry powder that produced a complete redispersion of ITZ nanoparticles in the aqueous solution. However,

the dry powder produced from ITZ nanosuspension without both mannitol and sodium taurocholate generated irreversible ITZ nanoparticle agglomerates. The latter and dry powder produced by spray-drying ITZ microparticles-based suspension with mannitol did not increase the ITZ C_s to above that of raw ITZ microparticles, which was below 10 ng mL^{-1} [53].

5.5.3 Nanoclusters

"Nanoclusters" are micron- or submicron-sized agglomerates of drug nanoparticles manufactured using an appropriate surfactant(s) and flocculating agent. Dry powders for inhalation are then obtained by employing a drying technique such as lyophilization.

Budesonide, having an aqueous solubility of ~15 μg mL^{-1} (Table 5.1), has been formulated as a suspension of nanoparticles of ~160–230 nm by a bottom-up precipitation technique [38]. Nanoclusters of ~2–4 μm were then produced by using an appropriate surfactant (lecithin) and flocculating agent (L-leucine). Nanoclusters were then lyophilized to produce dry powders with good aerodynamic performances (MMAD between 1.2 ± 0.04 and 1.6 ± 0.3 μm). In terms of the dissolution rate, the cumulative percentage of dissolved budesonide after 8 h was as follows: nanosuspension > nanoclusters > raw powder [38], in accordance with the decreasing specific surface area of the formulations. The same strategy was applied to PTX (Table 5.1), where the nanoclusters of PTX contained solubilized cisplatin in the dispersant media [62]. An improved dissolution rate of PTX was observed as follows: PTX nanoclusters containing cisplatin ≥ PTX nanosuspension > PTX nanoclusters not elaborated with cisplatin > raw PTX powder. The presence of the cisplatin (aqueous solubility ~1 mg mL^{-1}) in the PTX nanoclusters increased the dissolution rate of PTX to a level similar to that of PTX nanosuspension [62]. However, this tendency was not observed with other combinations of poorly water-soluble drug and soluble drug, such as fluticasone propionate (Table 5.1) and albuterol (aqueous solubility between 10 and 33 mg mL^{-1}) [49]. In this case, the presence of albuterol did not influence the dissolution rate, which was as follows: fluticasone propionate nanoparticles > fluticasone propionate nanoclusters with or without albuterol > raw fluticasone propionate powder [49].

5.6 Solid Dispersion/Amorphization

Solid dispersion of poorly water-soluble drugs in a highly hydrophilic carrier was first introduced into the pharmaceutical formulation area in 1961 by Sekiguchi and Obi [95]. It was thereafter used extensively as a strategy to increase drug solubility and, therefore, oral bioavailability of poorly water-soluble drugs [96]. SD is defined as a dispersion of one or more drugs in an inert carrier or matrix in the solid state, produced from a solution by the fusion, the solvent, or the fusion/solvent method [97]. A given SD is classified according to whether the drug is dispersed in the carrier at a molecular level, as a solid solution, or a glass solution (drug in a glassy carrier), or at a nonmolecular level, as a eutectic mixture (crystalline drug in crystalline carrier), as amorphous precipitation in a crystalline carrier (amorphous drug in crystalline carrier), as a glass suspension (amorphous/crystalline drug as a fine precipitate in a glassy carrier), or a combination of the preceding forms [97]. Solid solutions correspond to SDs, where the drug is dispersed in the carrier at a molecular level with complete miscibility/solubility (continuous solid solution) or incomplete miscibility/solubility (discontinuous solid solution). Eutectic mixtures are formed from two components that are miscible in the liquid state and immiscible in the solid state, leading to a dispersion of the drug as fine crystals, which improves wettability by the presence of the crystalline hydrophilic carrier. The most commonly developed SD system in the pharmaceutical field is the glass solution/suspension, which is a glass solution/dispersion where the glassy carrier (e.g., a polymer in an amorphous solid state) and the drug could be molecularly dispersed or form an amorphous drug precipitate into a glassy carrier

[98]. The latter system produces the highest enhancement in the dissolution of the drug because an amorphous drug is thermodynamically less stable than a crystalline one. The glassy carrier is usually a water-soluble sugar or polymer. Some surfactants can also be added to the system to enhance dissolution and/or prevent precipitation and/or agglomeration of drug [96]. The main potential problem associated with an SD containing an amorphous drug and/or carrier is the physical stability of the formulation. For example, crystallization during processing (mechanical stress) or during storage (temperature and humidity stress) might occur, which decreases the solubility and the dissolution rate of the drug [96].

The possible mechanisms of dissolution enhancement that result from SDs involve: (i) reduction in the drug particle size, which increases the surface area, (ii) changes in drug wettability brought about by modifying the surface characteristics of the drug particles (using surface active agents) or by using a highly hydrophilic carrier with direct dissolution or co-solvent effects, and (iii) formation of a higher energy solid-state form (e.g., amorphous form) of the drug, which requires a lower level of energy to break up the crystal lattice during the dissolution process and presents a higher aqueous solubility [99]. The actual mechanism(s) involved depend(s) on the specific SD formed.

TAC, having an aqueous solubility of ~20 μg mL^{-1} (Table 5.1), is defined as being a Class II drug by the BCS [70]. Moreover, TAC undergoes a high and variable metabolism, leading to an oral bioavailability ranging from 4% to 93% [64]. Raw TAC powder of 50–100 μm has been formulated with or without lactose using URF as a solvent method, and this generates a porous, nanostructured (from 100 to 200 nm in size) aggregate. The resultant formulations comprised either an SD of amorphous TAC in a lactose matrix (SD URF-TAC) or a crystalline TAC aggregate (URF-TAC) [64]. SD URF-TAC and URF-TAC presented significantly higher specific surface areas (29.3 and 25.9 m^2 g^{-1}), respectively, than the raw TAC powder (0.53 m^2 g^{-1}). These were delivered by nebulization and high FPDs were produced from the URF-based formulations. The percentage of dissolved TAC in SLF from the URF-based formulations was significantly higher than from raw TAC powder (72%, 67%, and 30% after 30 min for SD URF-TAC, URF-TAC, and raw TAC, respectively). The enhancement was attributed to the increase in the surface area and porosity provided by the nanostructured aggregates. Dissolution under supersaturated conditions showed an 11-fold higher solubility after 1 h from SD URF-TAC compared to that from URF-TAC, which in turn was close to the C_s of raw TAC powder in SLF. The supersaturated solubility then decreased to three times the C_s over the following 4 h, attaining the C_s only after 24 h. This large enhancement of C_s produced by SD URF-TAC is attributed to the high-energy phase of amorphous TAC particles and the presence of a hydrophilic carrier. *In vivo*, both lung and blood PKs showed a higher C_{max} and lower t_{max} for SD URF-TAC than for URF-TAC. These results suggest that the obtained supersaturation solubility increased the fraction of solubilized TAC that could not only exert its pharmacological action but also that is absorbed by diffusion through the lung epithelium into the blood [64].

The bioavailability of ITZ (Table 5.1), formulated as (i) a solid solution containing amorphous ITZ, mannitol, and lecithin [1:0.5:0.2 w/w/w] as nanostructured aggregates produced using URF (URF-ITZ) or (ii) as crystalline ITZ nanoparticles by wet milling (milled-ITZ) has been evaluated in rats, delivered by nebulization [51]. The SD (URF-ITZ) produced a supersaturated solution in SLF 4.7 times greater than that generated from crystalline ITZ nanoparticles (milled-ITZ) by an *in vitro* dissolution test carried out under saturation conditions. The superior solubility of the SD induced a higher plasma $AUC_{0-24\,h}$ for URF-ITZ versus milled ITZ (2543 ng h mL^{-1} vs. 662 ng h mL^{-1}, respectively) due to the increase in the dissolved dose of ITZ that can be absorbed through the lung tissue [51]. Both initially and 24 h after inhalation, the ITZ lung concentrations were similar from the nebulized URF-ITZ and milled-ITZ formulations. However, the SD seemed to provide a better formulation strategy for supersaturating the lung fluid and, therefore, potentiating the pharmacological action of the extremely poorly water-soluble ITZ (Table 5.1) in comparison to the use of nanocrystals. Nevertheless, the main clearance mechanism for URF-ITZ was absorption into the systemic compartment.

Duret *et al*. produced SD-based dry powders for inhalation by spray-drying hydro-isopropanolic solutions of ITZ and mannitol, with or without surfactants (TPGS or phospholipids). The resultant SDs, containing amorphous ITZ, generated both good aerodynamic and ITZ dissolution properties [55–57]. Both the amorphous state of ITZ and the presence of a hydrophilic matrix have been shown to increase significantly the dissolution profile in comparison to that which results from crystalline ITZ. Moreover, the inclusion of small amounts of surfactant (phospholipids or TPGS) in relation to the amorphous ITZ also has a positive influence on the dissolution rate [56, 57]. *In vitro* dissolution tests carried out under saturation conditions have demonstrated that a large increase in the C_s of ITZ can be achieved using the SD formulation in comparison to that obtained using raw crystalline ITZ. However, the supersaturation solubilities attained are relatively unstable over time and have ultimately tended to lower the equilibrium solubility. This resultant lower solubility was due to the remaining drug particles in contact with the dissolution medium recrystallizing into a lower energy, more stable form that possesses a lower C_s [57, 100]. A lung and systemic PK study was then conducted using the different dry powders delivered by endotracheal insufflation into mouse lungs [55]. The dry powders comprised: (i) micron-sized crystalline ITZ in crystalline mannitol (F1), (ii) SD of amorphous ITZ in crystalline mannitol (F2), or (iii) SD of amorphous ITZ and phospholipids in crystalline mannitol (F3). An *in vitro* dissolution test conducted under supersaturated conditions produced a large increase in aqueous solubility from below 10 ng mL^{-1} for the crystalline ITZ-based dry powder to a maximum of 498 ± 44 ng mL^{-1} or 450 ± 124 ng mL^{-1} for the SD dry powders with or without phospholipids, respectively (Figure 5.2A). This increase in solubility had a direct impact on the dissolution rate of ITZ from the SD dry powders (Figure 5.2B) and, therefore, also on the systemic PK profiles (Figure 5.2C). Indeed, plasma $AUC_{0-24\,h}$ from the SD dry powders with or without phospholipids were superior to that from the crystalline ITZ-based dry powder (376.8 ng h mL^{-1} and 491.5 ng h mL^{-1} vs. 182.0 ng h mL^{-1}, respectively) (Figure 5.2C). Moreover, plasma C_{max} values were higher (352 ± 119 ng mL^{-1} and 249 ± 54 ng mL^{-1} vs. 88 ± 11 ng mL^{-1}) and plasma t_{max}

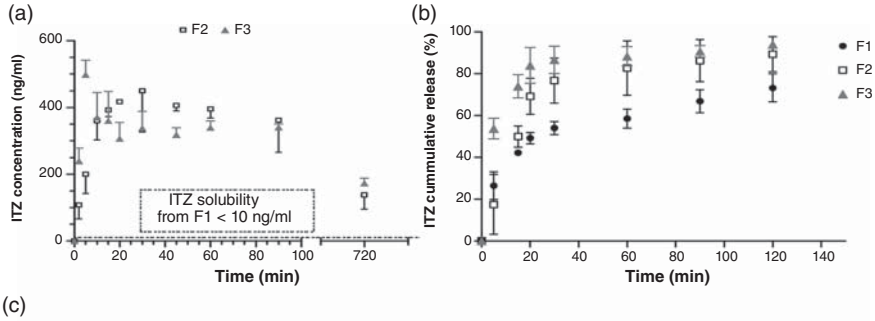

(c)

Itraconazole lung and plasma pharmacokinetic parameters after single endotracheal insufflation of formulations F1, F2, and F3.

	F1		F2		F3	
Administered dose	14.7 ± 5.1 (µg)		16.7 ± 2.5 (µg)		19.7 ± 4.2 (µg)	
	Lung	Plasma	Lung	Plasma	Lung	Plasma
C_{max}	35 ± 16 (µg/g)	88 ± 11 (ng/ml)	48 ± 14 (µg/g)	249 ± 54 (ng/ml)	46 ± 18 (µg/g)	352 ± 119 (ng/ml)
t_{max} (min)	–	60	–	30	–	5
AUC_{0-24h}	218.4 (µg h/g)	182.0 (ng h/ml)	332.6 (µg h/g)	491.5 (ng h/ml)	143.8 (µg h/g)	376.8 (ng h/ml)
AUC_{plasma} to AUC_{lung} ratio	8.3×10^{-4}		1.5×10^{-3}		2.6×10^{-3}	
k_{el} (h^{-1})	0.11	0.46	0.05	0.57	0.16	0.50
$t_{1/2el}$ (h)	6.5	1.5	14.7	1.2	4.1	1.4

Figure 5.2 *In vitro dissolution profiles in (A) supersaturation conditions (n=3, mean ± standard deviation) or (B) in "SINK" conditions (n=3, mean ± standard deviation) and (C) the lung and plasma pharmacokinetic parameters after endotracheal insufflation into mice lungs (n=5, mean ± standard deviation) of dry powders F1 (micron-sized crystalline ITZ in mannitol), F2 (SD with amorphous ITZ in mannitol) and F3 (SD with amorphous ITZ and phospholipids in mannitol) (Source: Reproduced from [55], with permission from Elsevier)*

values were lower (5 min and 30 min vs. 60 min) from the insufflated SD dry powders with or without phospholipids in comparison to the crystalline ITZ-based dry powder, respectively (Figure 5.2). The SD dry powder with phospholipids showed the highest plasma C_{max} after only 5 min, which was explained as being partly due to dissolution enhancement but particularly as a consequence of the permeation-enhancing property of phospholipids. This latter property drastically decreased the lung $t_{1/2}$ and finally induced the lowest lung $AUC_{0-24\,h}$ and lung tissue-to-serum concentration ratio. The SD dry powder without phospholipids presented the most appropriate PK properties for local drug delivery. Indeed, it presented the highest lung $AUC_{0-24\,h}$ and lung $t_{1/2,}$ with moderate plasma exposition (Figure 5.2) [55].

5.7 Micelles

Micelles are association or amphiphilic colloids that consist of two clearly distinct regions with opposite affinities toward a given solvent. They spontaneously form as potential drug carriers at certain concentrations in solution (i.e., the critical micelle concentration (CMC)) and temperature (i.e., the critical micellization temperature) from the aggregation of those amphiphilic agents (e.g., surfactants) [101]. Typically, in an aqueous medium, hydrophobic fragments of the amphiphilic molecules form the core of a micelle, while the hydrophilic fragments form the micelle's shell [101]. There is an enhancement in "apparent" solubility, as a consequence of solubilization of a poorly water-soluble drug within the hydrophobic interior via hydrophobic interaction or at the interface between the hydrophobic core and the hydrophilic shell of micelles by other molecular interactive forces. The benefit of the micellar solution arises mainly from the elimination of solid dissolution as a rate limiting step in the process of absorption [102]. The main mechanisms of drug release from a micelle are either diffusion from the core to the surrounding environment or due to micelle disintegration brought about by the dilution of the solution below the CMC [103]. Indeed, the use of this water miscible technology presents a higher risk of drug precipitation because dilution in biological media could decrease the solubilizing component concentration below the CMC and the otherwise poorly soluble drug could then precipitate [3]. Polymeric micelles have been formed from monomer units comprising both hydrophilic and hydrophobic regions. These micelles are more stable than those prepared from surfactants. This has been demonstrated by CMC values being approximately 1000-fold lower and their higher kinetic stability (i.e., the retarded disintegration of polymeric micelles at concentrations lower than CMC) [104]. In terms of tolerance by pulmonary tract, polymeric or nonpolymeric-based micelles have to be evaluated on a case by case for the biodegradability of the composite molecules, lack of inflammatory action, and noninterference with lung surfactant function.

There are now a large number of micelle-forming surfactants and newly developed amphiphilic polymers available for use as potential formulation excipients. Indeed, each polymer can be synthesized so as to contain a different number of monomer units, expanding the possible range even further [105]. Examples of amphiphilic polymers that can possibly be employed include lipid derivatives of water-soluble polymers (e.g., PEG-phosphatidylethanolamine and polyvinylpyrrolidone-palmityl or stearyl) [106]. The use of phospholipid moieties as hydrophobic blocks linked to hydrophilic polymer chains presents the advantage of higher particle stability. This stability is due to the existence of two fatty acid acyl groups in each phospholipid residue, which act so as to increase the hydrophobic interactions between the fatty acid chains in the micelle core [101]. Moreover, the presence of an enhanced level of mammalian secreted phospholipase A2 in inflammatory lung diseases [107] enables such molecules (including PEGylated phosphatidylethanolamine) to be degraded. Micelles generally have a spherical shape and exist in the nanometer dimension. Micelles could present a PEGylated shell, allow them to evade phagocytosis, and promote a better penetration of the mucus layer [108]. Micellization as a formulation strategy to increase the aqueous solubility of poorly water-soluble drugs has been tested for a number of drugs amenable to pulmonary delivery, including amphotericin B, BDP, budesonide, CSA, ITZ, and PTX (Table 5.1).

Amphotericin B is defined as a Class IV drug (poorly soluble and permeable) by the BCS system [70]. Therefore, only an increase in the aqueous solubility of amphotericin B would be expected to enhance its pharmacological action within the lung with limited absorptive clearance. A commercial form of amphotericin B solubilized in deoxycholate-based micelles (Fungizone®), designed for intravenous administration, contains amphotericin B at a much higher concentration than is possible in the absence of micelles. Indeed, sodium deoxycholate belongs to a class of biosurfactants called bile salts and its presence promotes the disaggregation of amphotericin B into monomeric and dimeric forms in the aqueous solution [109]. Using this technique, amphotericin B was solubilized to produce concentrations of 5 mg mL^{-1} in water (i.e., 20 000 times higher than the aqueous C_s of amphotericin B). Moreover, an *in vitro* dissolution test showed that 80% of amphotericin B was released within 24 h by diffusion, with the profile attaining a plateau for a further 48 h [110]. Ruijgrok *et al*. showed that aerosolization of 2 mg mL^{-1} of deoxycholate-micelle-based amphotericin B allowed 47 ± 16 $\mu g/g_{lung}$ of amphotericin B to be deposited in the lung after 60 min nebulization in healthy rats [111]. This deposited amount slightly decreased to 11 ± 3 $\mu g/g_{lung}$ after six weeks. The amphotericin B in blood was below detection levels for all samples, as might have been predicted due to its low permeability. These results demonstrate that there is a very low and slow absorptive clearance of amphotericin B, as reported by many research groups [112–114]. In addition, the effect on the mean minimum surface tension of the lung surfactant combined with amphotericin B in deoxycholate micelles or with deoxycholate micelles alone was evaluated [111]. A dose-dependent inhibition of the lung surfactant function with deoxycholate micelles with or without amphotericin B was observed, which was not observed with amphotericin B alone [111, 115]. Additionally, an increase in permeability and a decrease in the viability and integrity of Calu-3 monolayer cells were observed with amphotericin-B-based deoxycholate micelles [116]. To conclude, amphotericin B from deoxycholate micelles was eliminated very slowly from the lung and the absorption into the systemic circulation was also very low. However, amphotericin-B-based deoxycholate micelles, although apparently not well tolerated, have been tested in clinical trials, involving the nebulization of Fungizone® (Table 5.1) [24].

It has been reported that BDP, an inhaled corticosteroid used in asthma and chronic obstructive pulmonary disease, is likely to be removed from lower airways by mucociliary clearance prior to its dissolution and absorption, and partly swallowed into the gastrointestinal tract [117]. Therefore, Sahib *et al*. [35] solubilized BDP within polymeric micelles composed of a hydrophobic lung surfactant phospholipid, distearoyl phosphatidylethanolamine (DSPE) but with the latter PEGylated with hydrophilic PEG 5000 (DSPE-PEG_{5000}). An increase in apparent aqueous solubility (1300-fold higher than the C_s of BPD) was observed, and also a sustained release of BDP from the micelles was achieved, in comparison to that which occurred using raw BDP. Indeed, less than 41% of available BDP was released after 6 h from micelles in comparison to more than 90% for raw BDP during *in vitro* dissolution tests [35].

PTX has also been solubilized in DSPE-PEG_{5000} polymeric micelles and the formulation delivered by nebulization to rat lungs [61]. The reported CMC value of the polymer was very low, i.e., 6.4×10^{-6} M. An encapsulation efficiency above 95% was obtained with a PTX:DSPE-PEG_{5000} ratio of 1:40. The ultra-small size (5.0 ± 0.7 nm) of the micelles resulted in an increase in residence time in the lungs, probably due to both mucociliary clearance and alveolar macrophage phagocytosis mechanisms being evaded [118]. Thermal and RMN analysis showed that PTX formed a eutectic mixture with the polymer, i.e., PTX is dispersed molecularly inside the polymer matrix and more specifically within the core of the micelles. Unlike Taxol®, which is composed of surfactant-based micelles, the PTX release from PEG_{5000}-DSPE micelles was very low. Only 22% of PTX was released in SLF after 1 h, whereas more than 90% was released from Taxol® within the same time interval. The glassy core of PEG_{5000}-DSPE conferred less mobility on the drug, slowing down its diffusion, which resulted in a slow controlled release of PTX. Therefore, PEG_{5000}-DSPE micelles were more appropriate for local drug delivery in comparison to micelles of Taxol® because they increased the lung residence of PTX. Indeed, the lung $AUC_{0-12\,h}$ from PTX-based PEG_{5000}-DSPE micelles was threefold higher than that

from Taxol® (955 ± 52 vs. 317 ± 28 μg h g^{-1}). The ability of PEG_{5000}-DSPE micelles to control the release of PTX resulted in a lower plasma C_{max} of 73 ± 12 ng mL^{-1} at 6 h in comparison to a plasma C_{max} of 554 ± 19 ng mL^{-1} at 30 min from Taxol®, both delivered by the same intratracheal route. No inflammation was detected in BAL fluid as assessed by the low levels of both detectable alkaline phosphatase, a lysosomal enzyme indicating tissue damage, and β-N-acetylglucosaminidase, an enzyme secreted by alveolar macrophages, after repeated treatment with 100 mg kg^{-1} of PEG_{5000}-DSPE micelles for six consecutive days instilled in rat lungs [61]. The sustained release in the lung is explained by the low release profile of PTX from micelles, but certainly also by the slow degradation of the polymer by the pulmonary enzymes and the avoidance of alveolar macrophages and the mucociliary escalator [61, 119].

5.8 Liposomes

Liposomes are spherical lipid bilayered vesicles enclosing (an) aqueous compartment(s), which are classified according to their size and lamellarity [120]. Excipients used to produce liposomes are mainly lipids (such as phospholipids), sterols (mainly cholesterol), and fatty acids. In terms of tolerance, phospholipids and cholesterol are found in the membrane of body cells or in the lung surfactant. They are considered to present a high biocompatibility, since they are found to be biologically inert, with little antigenicity or pyrogenicity [85]. A poorly water-soluble drug can be solubilized in the lipid bilayer of liposomes according to its physicochemical properties, such as lipophilicity. Liposomes are known to sustain the release of poorly water-soluble drugs in the lung because the drug molecule has to be transferred from the liposome bilayer to the lung fluid prior to be absorbed. The rate of release depends on (i) liposome surface charge and size, (ii) the drug:lipid ratio, (iii) the composition and chain length of the phospholipid, and (iv) the presence of cholesterol or other excipients that affect membrane fluidity [85]. In the case of a drug that presents structural similarities with a lipid bilayer component, such as steroidal drugs with cholesterol, the main transfer route is (i) a flip–flop movement of the membrane component from the inner to the outlet leaflet (monolayer) of the donor membrane, (ii) departure of the membrane component from the membrane into the aqueous phase, (iii) association of the membrane component in the aqueous phase with the acceptor membrane, followed by (iv) a flip–flop to the inner membrane leaflet. However, most lipophilic drugs do not have a structural similarity with bilayer components and the main transfer steps are (i) dissolution of the drug in the lipid domain of the membrane, (ii) departure of the drug from the membrane into the aqueous phase, (iii) association of the drug component in the aqueous phase with the acceptor membrane, and (iv) dissolving of the drug in the acceptor membrane [43]. Moreover, there is less risk of drug precipitation by dilution in a biological medium (compared with its inclusion in micelles, for example), than when for example the drug is dissolved in a water-immiscible dispersed oil phase [3]. In the lung, the lipid components of liposomes can be rapidly entrapped in the lipid pool of the lung surfactant [85]. The latter is primarily composed of phospholipids (80%), mainly represented by dipalmitoyl phosphatidylcholine (DPPC), neutral lipids, such as cholesterol and fatty acids (8%), and proteins (12%). These components of the lung surfactant are mainly recycled by alveolar type II cells (90%) or cleared by alveolar macrophages (10%). Radiolabeled DPPC-based liposomes are rapidly associated with the lung surfactant and shown to follow the same recycling pathway [120]. Moreover, as a consequence of disease, an increase in mammalian secreted phospholipase A2 might be expected to accelerate the degradation of liposomal phospholipids. The rigidity of the liposome membrane or the use of PEGylated phospholipids increases the liposome stability in BAL [85].

Liposomal formulations for inhalation have been reviewed recently by Cipolla *et al*. [121]. Nebulization can affect several aspects of liposomes, such as their size and their membrane stability, and can also partly cause the release of the loaded drug. Liposomes presenting a higher gel–liquid crystal transition temperature (T_c) were found to be more stable during nebulization, with less alteration

occurring when a vibration mesh nebulizer was used [122]. Liposomes have also been delivered as a dry powder for inhalation [120, 121], but to date there is no liposomal product on the market for delivery via this route. Nevertheless, two late-stage clinical developments, Arikace®, a liposomal amikacin, and Pulmaquin®, a liposomal ciprofloxacin, might soon alter this situation [121].

Amphotericin B (Table 5.1) is known to transfer rapidly between lipid membranes. This transfer rate depends on the physical state (i.e., whether present in the gel state or liquid crystalline state) of the donor and the acceptor membranes [43]. Transfer is rapid between the donor DPPC-based liposomes and the acceptor liquid crystalline egg phosphatidylcholine liposomes only if the temperature is above the T_c of DPPC (i.e., 48 °C), when DPPC is in a liquid crystalline state [43]. In Ambisome®, amphotericin B is incorporated within the bilayer membrane of phospholipids, comprising small unilamellar vesicles. The drug forms an ion pair with the distearoyl phosphatidylglycerol (DSPG), in a molar ratio 1:2 (drug:DSPG). The liposomes are composed of hydrogenated soy phosphatidylcholine, cholesterol, DSPG, and amphotericin B (2:1:0.8:0.4 molar ratio), dispersed in a disodium succinate buffer and sucrose. These liposomes are composed of high T_c phospholipids and cholesterol, which slows down the amphotericin B transfer. Ruijgrok *et al*. showed that nebulized 4 mg mL^{-1} (i.e., 16 000-fold higher than the C_s of amphotericin B (Table 5.1)) liposomal amphotericin B (Ambisome®) allowed $26.9 \pm 8.5\ \mu g/g_{lung}$ of the drug to be deposited in the lungs after just a 60-min nebulization in healthy rats [111]. The dose remaining in the lungs decreased to $11.4 \pm 1.3\ \mu g/g_{lung}$ after six weeks, which was a slower loss than amphotericin B loaded in deoxycholate micelles (see Section 5.7 for more details). Moreover, no significant effect was seen on the mean minimal surface tension of the lung surfactant with amphotericin B alone or with liposomal amphotericin B, unlike when deoxycholate micelles were included within the formulation [111, 115, 123]. Moreover, liposomal amphotericin B showed a longer prophylactic protection than amphotericin B-based deoxycholate micelles. Indeed, both formulations presented a significant prophylactic efficacy when they were delivered two weeks before spore inoculation. However, only liposomal amphotericin B showed significant prophylactic efficacy when it was delivered six weeks before spore inoculation [111].

CSA is a cyclic undecapeptide immunosuppressant used to prevent lung rejection [44]. One molecule of CSA can be associated with 19 molecules of phospholipids through their acyl chains, which is the upper limit of CSA encapsulation in liposomal membranes [43, 124]. This association follows the classical "hydrophobic effect," which means that water molecules close to apolar solutes lose part of the rotational degree of freedom due to a lack of hydrogen bonding toward the apolar solutes [43]. CSA showed a propensity for bilayer exchange *in vivo*, inducing an apparent dissociation from dilauroyl phosphatidylcholine liposomes. Indeed, Arppe *et al*. have showed *in vivo* in mice that dilauroyl phosphatidylcholine-based liposomes loaded with CSA (7.5:1 w/w) delivered by nebulizer present a rapid dissociation between the CSA from the radiolabeled liposomes [125]. However, the lung $t_{1/2}$ proved to be 16.9 times longer for the radiolabeled liposomes than for CSA administered to healthy lungs (4.8 h vs. 17 min). Nevertheless, in inflamed lung, the lung $t_{1/2}$ decreased drastically and more specifically for the radiolabeled liposomes (2.2 h vs. 4.8 h) [125]. Trammer *et al*. [72] have determined apparent permeabilities from the apical to the basolateral side of human bronchial cell line Calu-3 monolayer for CSA encapsulated in 50 nm liposome and CSA dissolved in the culture medium. The apparent permeability of $0.96 \pm 0.04 \times 10^{-6}$ cm s^{-1} determined for liposomal CSA was lower than the $2.30 \pm 0.05 \times 10^{-6}$ cm s^{-1} for CSA solubilized in the culture medium. The CSA permeability was drastically decreased by using a liposome as a drug delivery system. Moreover, the transport of CSA from the liposomal formulation (0.50 ± 0.04 µg h cm^{-2}) across Calu-3 monolayers was lower than that from CSA alone in the culture medium (1.07 ± 0.05 µg h cm^{-2}). Liposomes are drug delivery systems that can extend the retention time of drug within the lung and can modify the PK of the encapsulated drug before its dissociation. However, in the case of CSA specifically, its high propensity for bilayer exchange limits the controlled release of the drug encapsulated in liposomes. Nevertheless, CSA liposomal formulations are much better tolerated in comparison to co-solvent formulations using ethanol or propylene glycol [71, 126].

5.9 Solid Lipid Nanoparticles and Nanostructured Lipid Carriers

A review of current research into lipidic micro- and nanoparticles for pulmonary delivery is given elsewhere (Chapter 6). Lipid nanoparticles are particulate systems generally sized within a 50–1000 nm range. The first generation comprised solid lipid nanoparticles (SLNs) derived from oil-in-water emulsions by replacing the liquid lipid (oil) with a solid lipid at body temperature [127]. These included only solid lipid(s) at body temperature, emulsifier(s) to stabilize them, and water as the dispersion medium [128, 129]. The lipids currently being advocated for use are natural, semisynthetic, or synthetic lipids such as triglycerides (e.g., tripalmitin), partial glycerides (e.g., glyceryl dibehenate known as Compritol® 888 ATO), fatty acids (e.g., stearic acid), steroids (e.g., cholesterol), and waxes (e.g., cetyl palmitate) [130]. Lipid nanoparticles can be produced by hot or cold HPH, according to the temperature sensitivity of the drug [127, 130]. Other techniques have been reported that use sonication or solvent diffusion/evaporation processes but such methods have the disadvantage that they are less transposable for scaling up production and/or use organic solvents [127, 128, 130].

The drug loading in lipid nanoparticles depends on (i) the drug solubility in melted lipid, (ii) the miscibility of drug melt and lipid melt, (iii) the chemical and physical structure of the solid lipid matrix, and (iv) the polymorphic state of the lipid material [127]. *In vitro* any prolonged release attained depends upon the lipid matrix, surfactant concentration, particle characteristics (e.g., size, porosity) and production parameters (e.g., temperature). For example, the burst effect which typically can occur from particulate systems depends mainly on the temperature and surfactant concentration and its ability to solubilize the drug [127]. Therefore, different drug incorporation models have been obtained such as: (i) a solid solution model (a homogeneous matrix where the API is molecularly dispersed or present as amorphous clusters in the lipid core with controlled-release properties if they are obtained by cold HPH), (ii) an API-enriched shell model without controlled-release properties, created by hot HPH when lipids recrystallize prior to API, and (iii) an API-enriched core model with controlled-release properties determined by the lipid shell, created by hot HPH when API recrystallizes prior to the lipids [127, 131]. During long-term storage, the drug can be expelled from the solid lipid matrix if the recrystallization of the lipid leads to highly crystalline particles with a perfect lattice (e.g., monoacid triglycerides) [127]. Indeed, the recrystallization of solid lipids during solidification often involves the formation of metastable polymorphs, which recrystallize using a time- and temperature-dependent transition into more stable forms [128]. With the aim of producing less perfect crystals with more imperfections offering spaces for drug and guaranteeing long-term physical stability during storage, a second generation of lipid nanoparticles appeared as nanostructured lipid carriers (NLCs). With such NLCs, the particles are produced from a blend of solid lipid(s) and liquid lipid(s), with the blend selected so as to remain solid at body temperature [129].

The phagocytosis of SLNs and/or NLCs by macrophages can be modulated following the use of appropriate surfactant, PEGylated phospholipids, or PEGylated fatty acids. For example, Poloxamine 908 has prevented the uptake of Compritol® SLN more efficiently than Poloxamer 407 [132]. In addition, the use of PEGylated dipalmitoyl phosphatidylethanolamine and PEGylated stearic acid to produce stealth SLNs has reduced the SLN uptake by murine macrophages to below that for the non-PEGylated SLN [133]. As regards potential tissue tolerance, lipids are assumed to be acceptable because they are found in living systems and possess their own metabolic pathways. However, the most critical excipient in terms of tolerance will be the choice of surfactant. Nassimi *et al*. [134] demonstrated that repeated inhalation exposure to SLN based on triglycerides and phospholipids stabilized by the polyethyleneglycol-15-hydroxystearate surfactant (Solutol® HS15) at a deposit dose below 200 µg did not induce tissue damage or inflammation in mouse lung [134]. Particles are subject to macrophage clearance, but Videira *et al*. [135] have showed that radiolabeled 200 nm SLNs based on Compritol® were mainly cleared by lymphatic drainage. SLNs and NLCs can either be delivered as an aqueous formulation by nebulization or as a dry powder by DPI [93], and these systems have

been reported to be more stable during nebulization than other systems, such as liposomes [93]. Clearly, these formulations may provide a useful approach that requires further investigation but at present no product for inhalation containing the SLNs or NLCs is marketed.

ITZ (Table 5.1) has been encapsulated in NLCs based on Precirol® ATO 5 and oleic acid (9:1) using hot HPH and stabilized with 2.5% polysorbate 20, producing particles with a drug loading of 0.4% [50]. Polysorbate 20 was selected as the surfactant so as to provide a compromise between stability and potential tolerance issues. The *in vitro* release of ITZ from the resultant NLCs was fast, with 80% released within 5 min. This rate suggests that the particles are best described by an API-enriched shell model. Nebulization of ITZ-based NLCs using a pneumatic and an ultrasonic device showed that no change in particle size, polydispersity index, or ITZ loading occurred during aerosolization [50]. However, no PK or biodistribution data have been reported with these ITZ-based NLCs.

CXB is a lipophilic COX-2-specific inhibitor defined as a Class II drug by the BCS [136]. It has been embedded in NLCs composed of Compritol® 888 ATO and Miglyol® 812 (triglycerides of caprylic and capric acid) by hot melt homogenization [42]. The CXB loading and the encapsulation efficiency were estimated at being 4% and 95.6%, respectively. *In vitro* controlled release of CXB from the NLCs was observed, with 8%–10% of CXB released after 8 h, 34% after 24 h, and more than 80% after 72 h in comparison to more than 95% after 8 h from a CXB solution. The nebulization of CXB NLCs using a jet nebulizer showed no change in particle size or CXB loading of the NLCs. The CXB solution and NLC suspension were then delivered to the mouse lung. The administration of CXB in NLCs resulted in a higher lung residence by maintaining concentration levels of the drug constant in the lung for 2 h, followed by a slow elimination until the concentration was below the limit of detection, 12 h after inhalation. The CXB solution was eliminated much faster, within 6 h after inhalation. Therefore, the lung $AUC_{0-24\,h}$ expressed in relation to the delivered dose was significantly higher for CXB NLCs in comparison to the CXB solution (1.26 vs. 0.36 μg h mL^{-1} $mg_{dose}{}^{-1}$, respectively). This change in lung residence produced alterations in the plasma profile of CXB, with longer plasma t_{max} (4.50 vs. 1.38 h) and higher plasma C_{max} values expressed in relation to the delivered dose (0.11 vs. 0.02 μg mL^{-1} $mg_{dose}{}^{-1}$) being obtained using the NLC suspension in comparison to the CXB solution [42]. These results for CXB NLCs in comparison to the CXB solution suggested the formation of a solid solution model. This model allowed the release of CXB to be controlled so as to increase the lung residence, as revealed by 3.5-fold higher lung $AUC_{0-24\,h}$. In addition, the NLCs increased the dissolved portion of the dose of CXB able to exert its pharmacological action and be absorbed in the blood, as revealed by the 22-fold higher plasma $AUC_{0-24\,h}$ [42].

5.10 Conclusion

Inhalation is a route of administration gaining interest for local as well as systemic drug delivery. Poorly water-soluble drugs now represent the major proportion of drugs both on the market and under development. Diverse well-known formulation strategies for poorly water-soluble drugs from the oral or parenteral route are now being applied to the pulmonary route. However, apart from the chemical modification of the initial drugs to form salts, polymorphs, or co-crystals, formulation strategies to improve aqueous solubility are greatly limited by the low number of excipients approved for pulmonary delivery. Moreover, contrary to systemic drug delivery, local drug delivery requires not only an increase in aqueous solubility but also controlled release for poorly soluble and highly permeable drugs to avoid rapid drug loss by absorptive clearance. Therefore, in this chapter, each formulation strategy has been briefly defined, explained, and illustrated with examples of studies using poorly water-soluble drugs intended for local lung delivery, as well as those used for systemic delivery. The examples chosen have been supported by *in vitro* dissolution and/or by *in vivo* lung and/or systemic PK data. Table 5.3 summarizes the advantages and disadvantages of each formulation strategy for

Table 5.3 *A summary of the possible formulation strategies under consideration for the inhaled delivery of poorly water-soluble drugs including possible excipients, ease of scale-up (+:easy, −:difficult), the improvement in aqueous solubility that is achievable (+++:high, ++:moderate, +:low), the in situ risk/release dependent on the lung environment, lung tolerance, and the risk of instability during long-term storage or inhalation*

Formulation strategies	Inhalation devices	Class of excipients	Scaling-up	Increase of solubility	*In situ*	Lung tolerance	Risk of instability
Co-solvent	Nebulizer, pMDI	Co-solvents	+	+++	Large risk of precipitation	Tissue irritation	/
Micronization	Nebulizer, pMDI, DPI	Surfactants, sugars	+	+	High nonabsorptive clearance	/	/
Nanocrystal suspension	Nebulizer, pMDI	Surfactants	+	++	Unstable supersaturation solubility	/	Poor stability during storage and nebulization
Nanocrystals in hydrophilic matrix	DPI	Sugars, surfactants	+	++	Unstable supersaturation solubility	/	/
Nanoclusters	DPI	Sugars, surfactants	+	++	Unstable supersaturation solubility	/	/
Solid dispersion (crystalline drug)	DPI	Sugars, polymers (surfactants)	+	++	Unstable supersaturation solubility	/	/
Solid dispersion (amorphous drug)	DPI	Sugars, polymers (surfactants)	+	+++	Unstable supersaturation solubility	/	+/− (amorphous stability)
Cyclodextrins	Nebulizer, pMDI, DPI	Cyclodextrins	+	++	Immediate release and stable supersaturation solubility	Could induce lung toxicity	/

PEGylation	Nebulizer, pMDI, DPI	PEG 2-5kDa	+	++	Could decrease lung permeability and recognition to alveolar macrophages	/	/
Surfactants-based micelles	Nebulizer	Surfactants	+	+++ (apparent solubility)	Disintegration of micelles by dilution and drug precipitation	Inhibition of lung surfactant function	/
Polymeric micelles	Nebulizer	Polymers (DSPE-PEG)	+	+++ (apparent solubility)	Sustained release by diffusion (DSPE-PEG)	Well tolerated (DSPE-PEG)	/
Liposomes	Nebulizer, DPI	Phospholipids, cholesterol, fatty acids	–	+++ (apparent solubility)	Sustained release limited by drug dissociation from liposome membrane	Biocompatible and well tolerated	Poor stability in lung and during nebulization
Solid lipid nanoparticles	Nebulizer, DPI	Solid lipids, surfactants	+	++ (apparent solubility)	Sustained release if solid solution or API-enriched core model	Could be well tolerated	Poor physical stability during storage and good stability by nebulization
Lipid nanocarriers	Nebulizer, DPI	Solid and liquid lipids, surfactants	+	+++ (apparent solubility)	Sustained release if solid solution or API-enriched core model	Could be well tolerated	High physical stability during storage and nebulization

pulmonary delivery. Formulations produced employing methodology that use excipients approved by FDA, considered as GRAS excipients for lung administration, or have already been commercially established, have the greater chance of reaching the market in the near future.

References

1. Williams, H.D., Trevaskis, N.L., Charman, S.A., *et al*. (2013). Strategies to address low drug solubility in discovery and development. *Pharmacological Reviews*, **65**(1), 315–499.
2. Shi, Y., Porter, W., Merdan, T. and Li, L.C. (2009). Recent advances in intravenous delivery of poorly water-soluble compounds. *Expert Opinion on Drug Delivery*, **6**(12), 1261–1282.
3. van Hoogevest, P., Liu, X. and Fahr, A. (2011). Drug delivery strategies for poorly water-soluble drugs: the industrial perspective. *Expert Opinion on Drug Delivery*, **8**(11), 1481–1500.
4. Amidon, G.L., Lennernas, H., Shah, V.P. and Crison, J.R. (1995). A theoretical basis for a biopharmaceutic drug classification: the correlation of in vitro drug product dissolution and in vivo bioavailability. *Pharmaceutical Research*, **12**(3), 413–420.
5. Labiris, N.R. and Dolovich, M.B. (2003). Pulmonary drug delivery. Part I: physiological factors affecting therapeutic effectiveness of aerosolized medications. *British Journal of Clinical Pharmacology*, **56**(6), 588–599.
6. Jain, K.K. (2008). Drug delivery systems – An overview. *Methods of Molecular Biology*, **437**, 1–50.
7. Patton, J.S., Fishburn, C.S. and Weers, J.G. (2004). The lungs as a portal of entry for systemic drug delivery. *Proceedings of the American Thoracic Society*, **1**(4), 338–344.
8. Pilcer, G. and Amighi, K. (2010). Formulation strategy and use of excipients in pulmonary drug delivery. *International Journal of Pharmaceutics*, **392**(1–2), 1–19.
9. Pilcer, G., Wauthoz, N. and Amighi, K. (2012). Lactose characteristics and the generation of the aerosol. *Advanced Drug Delivery Reviews*, **64**(3), 233–256.
10. Son, Y.-J., Mitchell, J.P. and McConville, J.T. (2011). In vitro performance testing for pulmonary drug delivery, in *Controlled Pulmonary Drug Delivery*, (eds. H.D.C. Smyth and A.J. Hickey), Springer, New York, pp. 383–415.
11. Noyes, A.A. and Whitney, W.R. (1897). The rate of solution of solid substances in their own solutions. *Journal of the American Chemical Society*, **19**, 930–934.
12. Einstein, A. (1905). Über die von der molekularkinetischen Theorie der Wärme geforderte Bewegung von in runhenden Flüssigkeiten suspendierten Teilchen. *Annall Physics*, **17**, 549.
13. Kirch, J., Guenther, M., Doshi, N., *et al*. (2012). Mucociliary clearance of micro- and nanoparticles is independent of size, shape and charge – an ex vivo and in silico approach. *Journal of Controlled Release*, **159**(1), 128–134.
14. Fischer, H. and Widdicombe, J.H. (2006). Mechanisms of acid and base secretion by the airway epithelium. *The Journal of Membrane Biology*, **211**(3), 139–150.
15. Ng, A.W., Bidani, A. and Heming, T.A. (2004). Innate host defense of the lung: effects of lung-lining fluid pH. *Lung*, **182**(5), 297–317.
16. Patton, J.S. (1996). Mechanisms of macromolecule absorption by the lungs. *Advanced Drug Delivery Reviews*, **19**, 3–36.
17. West, J.B. (2012). *Pulmonary Pathophysiology: The Essentials*, Wolters Kluwer Health: Philadelphia.
18. Lippmann, M. and Schlesinger, R.B. (1984). Interspecies comparisons of particle deposition and mucociliary clearance in tracheobronchial airways. *Journal of Toxicology and Environmental Health*, **13**(2–3), 441–469.
19. Munkholm, M. and Mortensen, J. (2013). Mucociliary clearance: pathophysiological aspects. *Clinical Physiology and Functional Imaging*, **34**, 171–177

20. Stone, K.C., Mercer, R.R., Gehr, P., *et al*. (1992). Allometric relationships of cell numbers and size in the mammalian lung. *American Journal of Respiratory Cell and Molecular Biology*, **6**(2), 235–243.
21. Ahsan, F., Rivas, I.P., Khan, M.A. and Torres Suarez, A.I. (2002). Targeting to macrophages: role of physicochemical properties of particulate carriers – liposomes and microspheres – on the phagocytosis by macrophages. *Journal of Controlled Release*, **79**(1–3), 29–40.
22. Forbes, B., Asgharian, B., Dailey, L.A., *et al*. (2011). Challenges in inhaled product development and opportunities for open innovation. *Advanced Drug Delivery Reviews*, **63**(1–2), 69–87.
23. Doan, T.V., Gregoire, N., Lamarche, I., *et al*. (2013). A preclinical PK modeling approach to the biopharmaceutical characterization of immediate and microsphere-based sustained release pulmonary formulations of rifampicin. *European Journal of Pharmaceutical Sciences*, **48**(1–2), 223–230.
24. Clinicaltrials.gov. (2014, January 9). Available from: http://www.clinicaltrials.gov.
25. Bates, D.W., Su, L., Yu, D.T., *et al*. (2001). Mortality and costs of acute renal failure associated with amphotericin B therapy. *Clinical Infectious Diseases*, **32**(5), 686–693.
26. Andes, D., Pascual, A. and Marchetti, O. (2009). Antifungal therapeutic drug monitoring: established and emerging indications. *Antimicrobial Agents and Chemotherapy*, **53**(1), 24–34.
27. Lass-Florl, C. (2011). Triazole antifungal agents in invasive fungal infections: a comparative review. *Drugs*, **71**(18), 2405–2419.
28. Denning, D.W., Lee, J.Y., Hostetler, J.S., *et al*. (1994). NIAID mycoses study group multicenter trial of oral itraconazole therapy for invasive aspergillosis. *The American Journal of Medicine*, **97**(2), 135–144.
29. Koshkina, N.V., Waldrep, J.C., Roberts, L.E., *et al*. (2001). Paclitaxel liposome aerosol treatment induces inhibition of pulmonary metastases in murine renal carcinoma model. *Clinical Cancer Research*, **7**(10), 3258–3262.
30. Videira, M., Almeida, A.J. and Fabra, A. (2012). Preclinical evaluation of a pulmonary delivered paclitaxel-loaded lipid nanocarrier antitumor effect. *Nanomedicine: Nanotechnology, Biology, and Medicine*, **8**(7), 1208–1215.
31. Gagnadoux, F., Hureaux, J., Vecellio, L., *et al*. (2008). Aerosolized chemotherapy. *Journal of Aerosol Medicine and Pulmonary Drug Delivery*, **21**(1), 61–70.
32. Fulzele, S.V., Chatterjee, A., Shaik, M.S., *et al*. (2006). Inhalation delivery and anti-tumor activity of celecoxib in human orthotopic non-small cell lung cancer xenograft model. *Pharmaceutical Research*, **23**(9), 2094–2106.
33. Zhang, J., Lv, H., Jiang, K. and Gao, Y. (2011). Enhanced bioavailability after oral and pulmonary administration of baicalein nanocrystal. *International Journal of Pharmaceutics*, **420**(1), 180–188.
34. Tolman, J.A. and Williams, R.O., 3rd., (2010). Advances in the pulmonary delivery of poorly water-soluble drugs: influence of solubilization on pharmacokinetic properties. *Drug Development and Industrial Pharmacy*, **36**(1), 1–30.
35. Sahib, M.N., Abdulameer, S.A., Darwis, Y., *et al*. (2012). Solubilization of beclomethasone dipropionate in sterically stabilized phospholipid nanomicelles (SSMs): physicochemical and in vitro evaluations. *Drug Design, Ddevelopment and Therapy*, **6**, 29–42.
36. Saari, M., Vidgren, M.T., Koskinen, M.O., *et al*. (1999). Pulmonary distribution and clearance of two beclomethasone liposome formulations in healthy volunteers. *International Journal of Pharmaceutics*, **181**(1), 1–9.
37. Cabral-Marques, H. and Almeida, R. (2009). Optimisation of spray-drying process variables for dry powder inhalation (DPI) formulations of corticosteroid/cyclodextrin inclusion complexes. *European Journal of Pharmaceutics and Biopharmaceutics*, **73**(1), 121–129.

38. El-Gendy, N., Gorman, E.M., Munson, E.J. and Berkland, C. (2009). Budesonide nanoparticle agglomerates as dry powder aerosols with rapid dissolution. *Journal of Pharmaceutical Sciences*, **98**(8), 2731–2746.
39. Sahib, M.N., Darwis, Y., Peh, K.K., *et al*. (2011). Rehydrated sterically stabilized phospholipid nanomicelles of budesonide for nebulization: physicochemical characterization and in vitro, in vivo evaluations. *International Journal of Nanomedicine*, **6**, 2351–2366.
40. Mezzena, M., Scalia, S., Young, P.M. and Traini, D. (2009). Solid lipid budesonide microparticles for controlled release inhalation therapy. *The AAPS Journal*, **11**(4), 771–778.
41. Joshi, M.R. and Misra, A. (2001). Liposomal budesonide for dry powder inhaler: preparation and stabilization. *AAPS PharmSciTech*, **2**(4), 25.
42. Patlolla, R.R., Chougule, M., Patel, A.R., *et al*. (2010). Formulation, characterization and pulmonary deposition of nebulized celecoxib encapsulated nanostructured lipid carriers. *Journal of Controlled Release*, **144**(2), 233–241.
43. Fahr, A., van Hoogevest, P., May, S., *et al*. (2005). Transfer of lipophilic drugs between liposomal membranes and biological interfaces: consequences for drug delivery. *European Journal of Pharmaceutical Sciences*, **26**(3–4), 251–265.
44. Niven, R.W. (2011). Toward managing chronic rejection after lung transplant: the fate and effects of inhaled cyclosporine in a complex environment. *Advanced Drug Delivery Reviews*, **63**(1–2), 88–109.
45. Taljanski, W., Pierzynowski, S.G., Lundin, P.D., *et al*. (1997). Pulmonary delivery of intratracheally instilled and aerosolized cyclosporine A to young and adult rats. *Drug Metabolism and Disposition*, **25**(8), 917–920.
46. Zijlstra, G.S., Rijkeboer, M., Jan van Drooge, D., *et al*. (2007). Characterization of a cyclosporine solid dispersion for inhalation. *The AAPS Journal*, **9**(2), E190–199.
47. Tam, J.M., McConville, J.T., Williams, R.O., 3rd, and Johnston, K.P. (2008). Amorphous cyclosporin nanodispersions for enhanced pulmonary deposition and dissolution. *Journal of Pharmaceutical Sciences*, **97**(11), 4915–4933.
48. Yamasaki, K., Kwok, P.C., Fukushige, K., *et al*. (2011). Enhanced dissolution of inhalable cyclosporine nano-matrix particles with mannitol as matrix former. *International Journal of Pharmaceutics*, **420**(1), 34–42.
49. El-Gendy, N., Pornputtapitak, W. and Berkland, C. (2011). Nanoparticle agglomerates of fluticasone propionate in combination with albuterol sulfate as dry powder aerosols. *European Journal of Pharmaceutical Sciences*, **44**(4), 522–533.
50. Pardeike, J., Weber, S., Haber, T., *et al*. (2011). Development of an itraconazole-loaded nanostructured lipid carrier (NLC) formulation for pulmonary application. *International Journal of Pharmaceutics*, **419**(1–2), 329–338.
51. Yang, W., Johnston, K.P. and Williams, R.O., 3rd., (2010). Comparison of bioavailability of amorphous versus crystalline itraconazole nanoparticles via pulmonary administration in rats. *European Journal of Pharmaceutics and Biopharmaceutics*, **75**(1), 33–41.
52. Rundfeldt, C., Steckel, H., Scherliess, H., *et al*. (2013). Inhalable highly concentrated itraconazole nanosuspension for the treatment of bronchopulmonary aspergillosis. *European Journal of Pharmaceutics and Biopharmaceutics*, **83**(1), 44–53.
53. Duret, C., Wauthoz, N., Sebti, T., *et al*. (2012). New inhalation-optimized itraconazole nanoparticle-based dry powders for the treatment of invasive pulmonary aspergillosis. *International Journal of Nanomedicine*, **7**, 5475–5489.
54. Yang, W., Tam, J., Miller, D.A., *et al*. (2008). High bioavailability from nebulized itraconazole nanoparticle dispersions with biocompatible stabilizers. *International Journal of Pharmaceutics*, **361**(1–2), 177–188.
55. Duret, C., Merlos, R., Wauthoz, N., *et al*. (2014). Pharmacokinetic evaluation in mice of amorphous itraconazole-based dry powder formulations for inhalation with high bioavailability and

extended lung retention. *European Journal of Pharmaceutics and Biopharmaceutics.* **86**(1), 46–64.

56. Duret, C., Wauthoz, N., Sebti, T., *et al*. (2012). New respirable and fast dissolving itraconazole dry powder composition for the treatment of invasive pulmonary aspergillosis. *Pharmaceutical Research*, **29**(10), 2845–2859.
57. Duret, C., Wauthoz, N., Sebti, T., *et al*. (2012). Solid dispersions of itraconazole for inhalation with enhanced dissolution, solubility and dispersion properties. *International Journal of Pharmaceutics*, **428**(1–2), 103–113.
58. Yang, W., Chow, K.T., Lang, B., *et al*. (2010). In vitro characterization and pharmacokinetics in mice following pulmonary delivery of itraconazole as cyclodextrin solubilized solution. *European Journal of Pharmaceutical Sciences*, **39**(5), 336–347.
59. Moazeni, E., Gilani, K., Najafabadi, A.R., *et al*. (2012). Preparation and evaluation of inhalable itraconazole chitosan based polymeric micelles. *Daru*, **20**(1), 85.
60. Surapaneni, M.S., Das, S.K. and Das, N.G. (2012). Designing Paclitaxel drug delivery systems aimed at improved patient outcomes: current status and challenges. *ISRN Pharmacology*, **2012**, 623139.
61. Gill, K.K., Nazzal, S. and Kaddoumi, A. (2011). Paclitaxel loaded PEG(5000)-DSPE micelles as pulmonary delivery platform: formulation characterization, tissue distribution, plasma pharmacokinetics, and toxicological evaluation. *European Journal of Pharmaceutics and Biopharmaceutics*, **79**(2), 276–284.
62. El-Gendy, N. and Berkland, C. (2009). Combination chemotherapeutic dry powder aerosols via controlled nanoparticle agglomeration. *Pharmaceutical Research*, **26**(7), 1752–1763.
63. Hureaux, J., Lagarce, F., Gagnadoux, F., *et al*. (2009). Lipid nanocapsules: ready-to-use nanovectors for the aerosol delivery of paclitaxel. *European Journal of Pharmaceutics and Biopharmaceutics*, **73**(2), 239–246.
64. Sinswat, P., Overhoff, K.A., McConville, J.T., *et al*. (2008). Nebulization of nanoparticulate amorphous or crystalline tacrolimus – single-dose pharmacokinetics study in mice. *European Journal of Pharmaceutics and Biopharmaceutics*, **69**(3), 1057–1066.
65. Beinborn, N.A., Du, J., Wiederhold, N.P., *et al*. (2012). Dry powder insufflation of crystalline and amorphous voriconazole formulations produced by thin film freezing to mice. *European Journal of Pharmaceutics and Biopharmaceutics*, **81**(3), 600–608.
66. Tolman, J.A., Nelson, N.A., Son, Y.J., *et al*. (2009). Characterization and pharmacokinetic analysis of aerosolized aqueous voriconazole solution. *European Journal of Pharmaceutics and Biopharmaceutics*, **72**(1), 199–205.
67. FDA. (2014, January 9). Available from: http://www.accessdata.fda.gov/scripts/cder/IIG/.
68. Lewis, D.A., Young, P.M., Buttini, F., *et al*. (2013). Towards the bioequivalence of pressurized metered dose inhalers 1: Design and characterisation of aerodynamically equivalent beclomethasone dipropionate inhalers with and without glycerol as a non-volatile excipient. *European Journal of Pharmaceutics and Biopharmaceutics.* **86**, 31–37.
69. Trivedi, J.S. and Wells, M.L. (2000). Solubilization using Cosolvent Approach, in Water-Insoluble Drug Formulation, (ed. R. Liu), Interpharm Press, Denver, pp. 141–168.
70. Wu, C.Y. and Benet, L.Z. (2005). Predicting drug disposition via application of BCS: transport/absorption/ elimination interplay and development of a biopharmaceutics drug disposition classification system. *Pharmaceutical Research*, **22**(1), 11–23.
71. Corcoran, T.E. (2006). Inhaled delivery of aerosolized cyclosporine. *Advanced Drug Delivery Reviews*, **58**(9–10), 1119–1127.
72. Trammer, B., Amann, A., Haltner-Ukomadu, E., *et al*. (2008). Comparative permeability and diffusion kinetics of cyclosporine A liposomes and propylene glycol solution from human lung tissue into human blood ex vivo. *European Journal of Pharmaceutics and Biopharmaceutics*, **70**(3), 758–764.

73. Burkart, G.J., Smaldone, G.C., Eldon, M.A., *et al*. (2003). Lung deposition and pharmacokinetics of cyclosporine after aerosolization in lung transplant patients. *Pharmaceutical Research*, **20**(2), 252–256.
74. Brewster, M.E. and Loftsson, T. (2007). Cyclodextrins as pharmaceutical solubilizers. *Advanced Drug Delivery Reviews*, **59**(7), 645–666.
75. Stella, V.J. and He, Q. (2008). Cyclodextrins. *Toxicologic Pathology*, **36**(1), 30–42.
76. Matilainen, L., Toropainen, T., Vihola, H., *et al*. (2008). In vitro toxicity and permeation of cyclodextrins in Calu-3 cells. *Journal of Controlled Release*, **126**(1), 10–16.
77. Marques, H.M.C., Hadgraft, J., Kellaway, I.W. and Taylor, G. (1991). Studies of cyclodextrin inclusion complexes. III. The pulmonary absorption of β-, DM-β- and HP-β-cyclodextrins in rabbits. *International Journal of Pharmaceutics*, **77**, 297–302.
78. Salem, L.B., Bosquillon, C., Dailey, L.A., *et al*. (2009). Sparing methylation of beta-cyclodextrin mitigates cytotoxicity and permeability induction in respiratory epithelial cell layers in vitro. *Journal of Controlled Release*, **136**(2), 110–116.
79. Mathia, N.R., Timoszyk, J., Stetsko, P.I., *et al*. (2002). Permeability characteristics of calu-3 human bronchial epithelial cells: in vitro–in vivo correlation to predict lung absorption in rats. *Journal of Drug Targeting*, **10**(1), 31–40.
80. Piel, G., Piette, M., Barillaro, V., *et al*. (2007). Study of the relationship between lipid binding properties of cyclodextrins and their effect on the integrity of liposomes. *International Journal of Pharmaceutics*, **338** (1–2), 35–42.
81. Evrard, B., Bertholet, P., Gueders, M., *et al*. (2004). Cyclodextrins as a potential carrier in drug nebulization. *Journal of Controlled Release*, **96**(3), 403–410.
82. Fishburn, C.S. (2008). The pharmacology of PEGylation: balancing PD with PK to generate novel therapeutics. *Journal of Pharmaceutical Sciences*, **97**(10), 4167–4183.
83. Pasut, G. and Veronese, F.M. (2009). PEG conjugates in clinical development or use as anticancer agents: an overview. *Advanced Drug Delivery Reviews*, **61**(13), 1177–1188.
84. Caliceti, P. and Veronese, F.M. (2003). Pharmacokinetic and biodistribution properties of poly(ethylene glycol)-protein conjugates. *Advanced Drug Delivery Reviews*, **55**(10), 1261–1277.
85. Sheth, P. and Myrdal, P.B. (2011). Excipients utilized for modifying pulmonary drug release, in *Controlled Pulmonary Drug Delivery*, (eds. H.D.C. Smyth and A.J. Hickey), Springer, New York, pp. 237–263.
86. Youn, Y.S., Kwon, M.J., Na, D.H., *et al*. (2008). Improved intrapulmonary delivery of site-specific PEGylated salmon calcitonin: optimization by PEG size selection. *Journal of Controlled Release*, **125**(1), 68–75.
87. Wattendorf, U. and Merkle, H.P. (2008). PEGylation as a tool for the biomedical engineering of surface modified microparticles. *Journal of Pharmaceutical Sciences*, **97**(11), 4655–4669.
88. Amoozgar, Z. and Yeo, Y. (2012). Recent advances in stealth coating of nanoparticle drug delivery systems. *Wiley Interdisciplinary Reviews. Nanomedicine and Nanobiotechnology*, **4**(2), 219–233.
89. Suk, J.S., Lai, S.K., Wang, Y.Y., *et al*. (2009). The penetration of fresh undiluted sputum expectorated by cystic fibrosis patients by non-adhesive polymer nanoparticles. *Biomaterials*, **30**(13), 2591–2597.
90. Klonne, D.R., Dodd, D.E., Losco, P.E., *et al*. (1989). Two-week aerosol inhalation study on polyethylene glycol (PEG) 3350 in F-344 rats. *Drug and Chemical Toxicology*, **12**(1), 39–48.
91. Junghanns, J.U. and Muller, R.H. (2008). Nanocrystal technology, drug delivery and clinical applications. *International Journal of Nanomedicine*, **3**(3), 295–309.
92. O'Riordan, T.G. (2002). Formulations and nebulizer performance. *Respiratory Care*, **47**(11), 1305–1312; discussion 1312–1303.

93. Weber, S., Zimmer, A. and Pardeike, J. (2013). Solid lipid nanoparticles (SLN) and nanostructured lipid carriers (NLC) for pulmonary application: a review of the state of the art. *European Journal of Pharmaceutics and Biopharmaceutics.* **86**, 7–22.
94. Groneberg, D.A., Witt, C., Wagner, U., *et al*. (2003). Fundamentals of pulmonary drug delivery. *Respiratory Medicine*, **97**(4), 382–387.
95. Sekiguchi, K. and Obi, N. (1961). Studies on absorption of eutectic mixtures. *I. A comparison of the behavior of eutectic mixture of sulfathiazole and that of ordinary sulfathiazole in man. Chemical and Pharmaceutical Bulletin*, **9**(11), 866–872.
96. Vasconcelos, T., Sarmento, B. and Costa, P. (2007). Solid dispersions as strategy to improve oral bioavailability of poor water soluble drugs. *Drug Discovery Today*, **12**(23–24), 1068–1075.
97. Chiou, W.L. and Riegelman, S. (1971). Pharmaceutical applications of solid dispersion systems. *Journal of Pharmaceutical Sciences*, **60**(9), 1281–1302.
98. Janssens, S. and Van den Mooter, G. (2009). Review: physical chemistry of solid dispersions. *The Journal of Pharmacy and Pharmacology*, **61**(12), 1571–1586.
99. Nanda, A.R., Rowling, C.E., Barker, N.P. and Sheen, P.-C. (2000). Immediate release solid dispersions for oral drug delivery, in *Water-Insoluble Drug Formulation*, (ed. R. Liu), Interpharm Press, Denver, pp. 493–523.
100. Freiwald, M., Valotis, A., Kirschbaum, A., *et al*. (2005). Monitoring the initial pulmonary absorption of two different beclomethasone dipropionate aerosols employing a human lung reperfusion model. *Respiratory Research*, **6**, 21.
101. Torchilin, V.P. (2007). Micellar nanocarriers: pharmaceutical perspectives. *Pharmaceutical Research*, **24**(1), 1–16.
102. Liu, R., Sadrzadeh, N. and Constantinides, P.P. (2000). Micellization and drug solubility enhancement, in *Water-insoluble Drug Formulation*, (ed. R. Liu), Interpharm Press: Denver, pp. 213–354.
103. Soo, P.L., Liu, J., Allen, C., *et al*. (2006). *Polymeric micelles for formulation of anticancer drugs*, in *Nanotechnology for Cancer Therapy*, (ed. M.M. Amiji), Floride, pp. 317–355.
104. Owen, S.C., Chan, D.P.Y. and Shoichet, M.S. (2012). Polymeric micelle stability. *Nano Today*, **7**(1), 53–65.
105. Kedar, U., Phutane, P., Shidhaye, S. and Kadam, V. (2010). Advances in polymeric micelles for drug delivery and tumor targeting. *Nanomedicine: Nanotechnology, Biology, and Medicine*, **6**(6), 714–729.
106. Lukyanov, A.N. and Torchilin, V.P. (2004). Micelles from lipid derivatives of water-soluble polymers as delivery systems for poorly soluble drugs. *Advanced Drug Delivery Reviews*, **56**(9), 1273–1289.
107. Granata, F., Nardicchi, V., Loffredo, S., *et al*. (2009). Secreted phospholipases A(2): A proinflammatory connection between macrophages and mast cells in the human lung. *Immunobiology*, **214**(9–10), 811–821.
108. Smola, M., Vandamme, T. and Sokolowski, A. (2008). Nanocarriers as pulmonary drug delivery systems to treat and to diagnose respiratory and non respiratory diseases. *International Journal of Nanomedicine*, **3**(1), 1–19.
109. Selvam, S. and Mishra, A.K. (2008). Disaggregation of amphotericin B by sodium deoxycholate micellar aggregates. *Journal of Photochemistry and Photobiology. B: Biology*, **93**(2), 66–70.
110. Jain, J.P. and Kumar, N. (2010). Development of amphotericin B loaded polymersomes based on (PEG)(3)-PLA co-polymers: factors affecting size and in vitro evaluation. *European Journal of Pharmaceutical Sciences*, **40**(5), 456–465.
111. Ruijgrok, E.J., Fens, M.H., Bakker-Woudenberg, I.A., *et al*. (2005). Nebulization of four commercially available amphotericin B formulations in persistently granulocytopenic rats with invasive pulmonary aspergillosis: evidence for long-term biological activity. *The Journal of Pharmacy and Pharmacology*, **57**(10), 1289–1295.

112. Koizumi, T., Kubo, K., Kaneki, T., *et al*. (1998). Pharmacokinetic evaluation of amphotericin B in lung tissue: lung lymph distribution after intravenous injection and airspace distribution after aerosolization and inhalation of amphotericin B. *Antimicrobial Agents and Chemotherapy*, **42**(7), 1597–1600.
113. Niki, Y., Bernard, E.M., Schmitt, H.J., *et al*. (1990). Pharmacokinetics of aerosol amphotericin B in rats. *Antimicrobial Agents and Chemotherapy*, **34**(1), 29–32.
114. Lowry, C.M., Marty, F.M., Vargas, S.O., *et al*. (2007). Safety of aerosolized liposomal versus deoxycholate amphotericin B formulations for prevention of invasive fungal infections following lung transplantation: a retrospective study. *Transplant Infectious Disease: An Official Journal of the Transplantation Society*, **9**(2), 121–125.
115. Ruijgrok, E.J., Vulto, A.G. and Van Etten, E.W. (2001). Efficacy of aerosolized amphotericin B desoxycholate and liposomal amphotericin B in the treatment of invasive pulmonary aspergillosis in severely immunocompromised rats. *The Journal of Antimicrobial Chemotherapy*, **48**(1), 89–95.
116. Burgess, B.L., Cavigiolio, G., Fannucchi, M.V., *et al*. (2010). A phospholipid-apolipoprotein A-I nanoparticle containing amphotericin B as a drug delivery platform with cell membrane protective properties. *International Journal of Pharmaceutics*, **399**(1–2), 148–155.
117. Sakagami, M., Kinoshita, W., Sakon, K., *et al*. (2002). Mucoadhesive beclomethasone microspheres for powder inhalation: their pharmacokinetics and pharmacodynamics evaluation. *Journal of Controlled Release*, **80**(1–3), 207–218.
118. Oberdorster, G. (2001). Pulmonary effects of inhaled ultrafine particles. *International Archives of Occupational and Environmental Health*, **74**(1), 1–8.
119. Pepic, I., Lovric, J. and Filipovic-Grcic, J. (2013). How do polymeric micelles cross epithelial barriers? *European Journal of Pharmaceutical Sciences*, **50**(1), 42–55.
120. Swaminathan, J. and Ehrhardt, C. (2011). Liposomes for pulmonary drug delivery, In *Controlled Pulmonary Drug Delivery*, (eds. H.D.C. Smyth and A.J. Hickey), Springer, New York, pp. 313–334.
121. Cipolla, D., Gonda, I. and Chan, H.K. (2013). Liposomal formulations for inhalation. *Therapeutic Delivery*, **4**(8), 1047–1072.
122. Kleemann, E., Schmehl, T., Gessler, T., *et al*. (2007). Iloprost-containing liposomes for aerosol application in pulmonary arterial hypertension: formulation aspects and stability. *Pharmaceutical Research*, **24**(2), 277–287.
123. Griese, M., Schams, A. and Lohmeier, K.P. (1998). Amphotericin B and pulmonary surfactant. *European Journal of Medical Research*, **3**(8), 383–386.
124. Ouyang, C., Choice, E., Holland, J., *et al*. (1995). Liposomal cyclosporine. Characterization of drug incorporation and interbilayer exchange. *Transplantation*, **60**(9), 999–1006.
125. Arppe, J., Vidgren, M. and Waldrep, J.C. (1998). Pulmonary pharmacokinetics of cyclosporin A liposomes. *International Journal of Pharmaceutics*, **161**(2), 205–214.
126. Gilbert, B.E., Knight, C., Alvarez, F.G., *et al*. (1997). Tolerance of volunteers to cyclosporine A-dilauroylphosphatidylcholine liposome aerosol. *American Journal of Respiratory and Critical Care Medicine*, **156**(6), 1789–1793.
127. Muller, R.H., Mader, K. and Gohla, S. (2000). Solid lipid nanoparticles (SLN) for controlled drug delivery – a review of the state of the art. *European Journal of Pharmaceutics and Biopharmaceutics*, **50**(1), 161–177.
128. Bunjes, H. (2010). Lipid nanoparticles for the delivery of poorly water-soluble drugs. *The Journal of Pharmacy and Pharmacology*, **62**(11), 1637–1645.
129. Muller, R.H., Petersen, R.D., Hommoss, A. and Pardeike, J. (2007). Nanostructured lipid carriers (NLC) in cosmetic dermal products. *Advanced Drug Delivery Reviews*, **59**(6), 522–530.
130. Mehnert, W. and Mader, K. (2001). Solid lipid nanoparticles: production, characterization and applications. *Advanced Drug Delivery Reviews*, **47**(2–3), 165–196.

131. Souto, E.B. and Müller, R.H. (2010). Lipid nanoparticles: effect on bioavailability and pharmacokinetic changes, in *Drug Delivery*, (ed. M. Schäfer-Korting), Springer, Berlin Heidelberg, pp. 115–141.
132. Müller, R.H. and Olbrich, C. (1999). Solid lipid nanoparticles: phagocytic uptake, in vitro cytotoxicity and in vivo biodegradation 1st communication. *Pharm Ind*, **61**, 462–467.
133. Bocca, C., Caputo, O., Cavalli, R., *et al*. (1998). Phagocytic uptake of fluorescent stealth and non-stealth solid lipid nanoparticles. *International Journal of Pharmaceutics*, **175**, 185–193.
134. Nassimi, M., Schleh, C., Lauenstein, H.D., *et al*. (2010). A toxicological evaluation of inhaled solid lipid nanoparticles used as a potential drug delivery system for the lung. *European Journal of Pharmaceutics and Biopharmaceutics*, **75**(2), 107–116.
135. Videira, M.A., Gano, L., Santos, C., *et al*. (2006). Lymphatic uptake of lipid nanoparticles following endotracheal administration. *Journal of Microencapsulation*, **23**(8), 855–862.
136. BCS. (2014 January 9). Available from: http://166.78.14.201/tsrlinc.com/services/bcs/results.cfm.